Parity Violation program at MESA

Frank Maas

MITP workshop:
Precision Tests with Neutral-Current Coherent Interactions with Nuclei

Johannes Gutenberg Universität Mainz
May 23 – May 27, 2022

Outline:

- Physics motivation
- Experimental Method
- Experimental Program
- Neutron Skin in Project: Talk by Michaela Thiel on Wednesday

Physics motivation

Search for New Physics: Various Methods

Direct: High Energy (LHC)

Indirect: High Precision

Anom. Mag. Moment

$(g\text{-}2)_{\mu,e}$, EDM, $\sin^2\theta_W$, …

Indirect: High Intensity

Rare B-decays

R_{D^*}

at low energy,

accurate theory needed

Direct observation versus precision measurements: top-quark, Higgs

Direct measurement

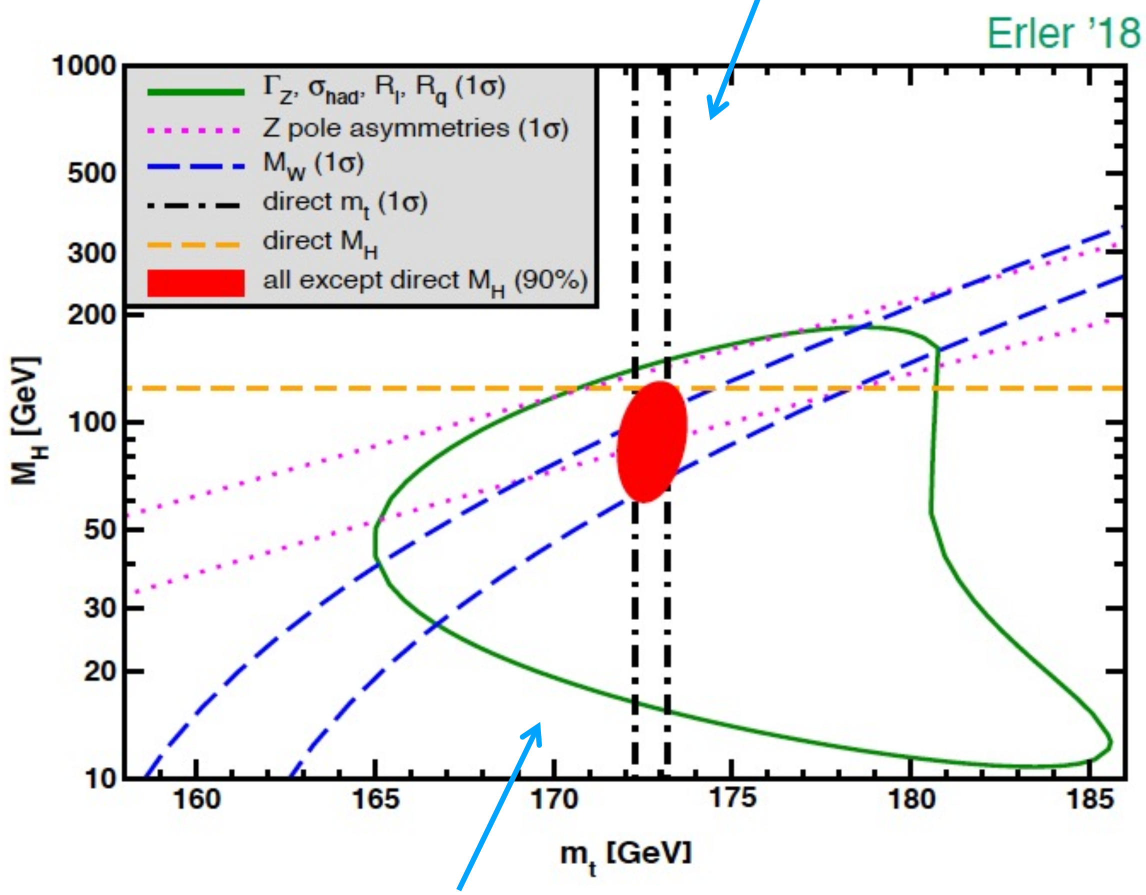

Direct measurements:

$M_{\rm H} = 125.14 \pm 0.15$ GeV

$m_{\rm t} = 172.74 \pm 0.46$ GeV

Indirect prediction:

$M_{\rm H} = 90^{+17}_{-16}$ GeV

$m_{\rm t} = 176.4 \pm 1.8$ GeV

Indirect measurements

Weak mixing angle

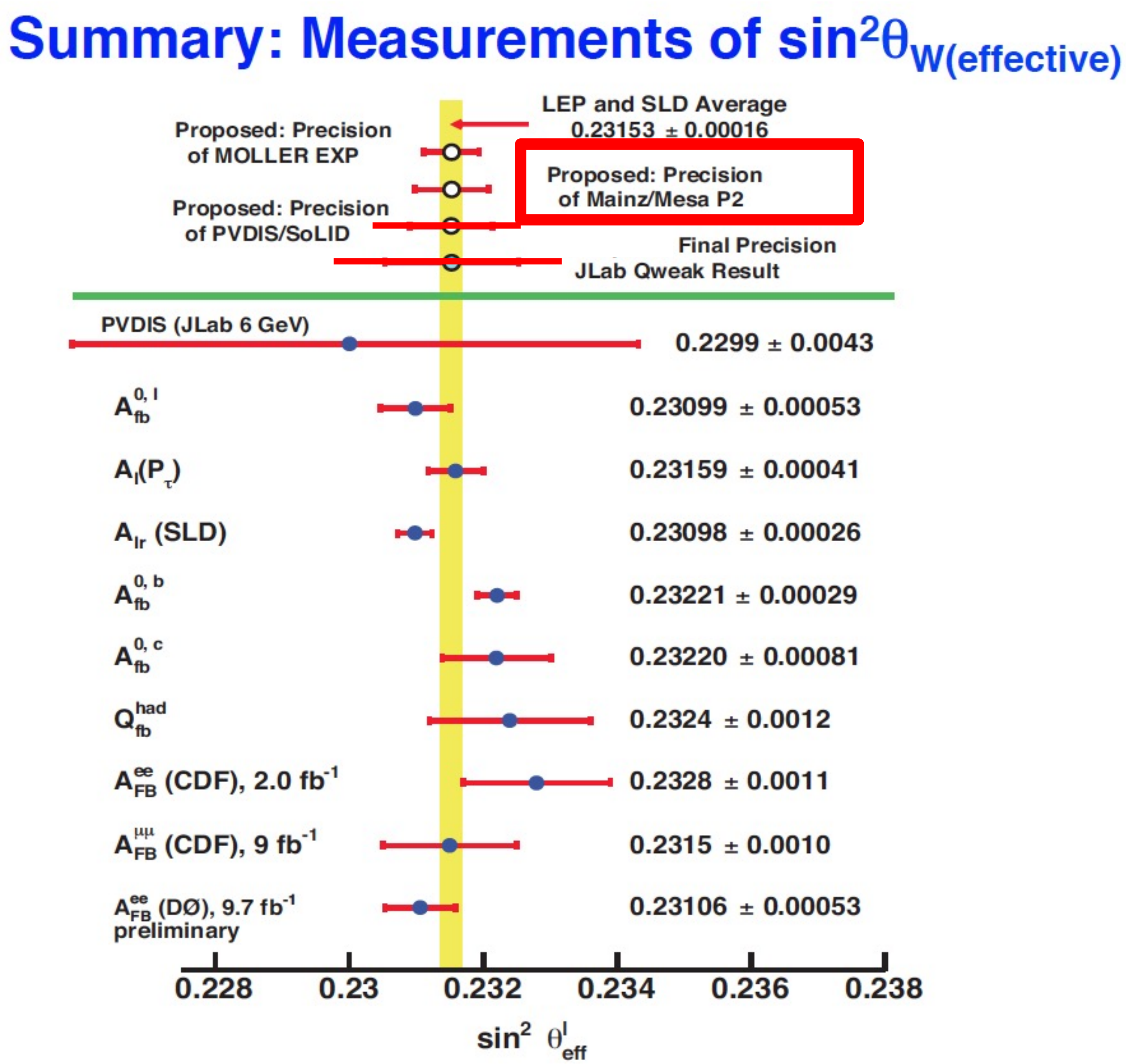

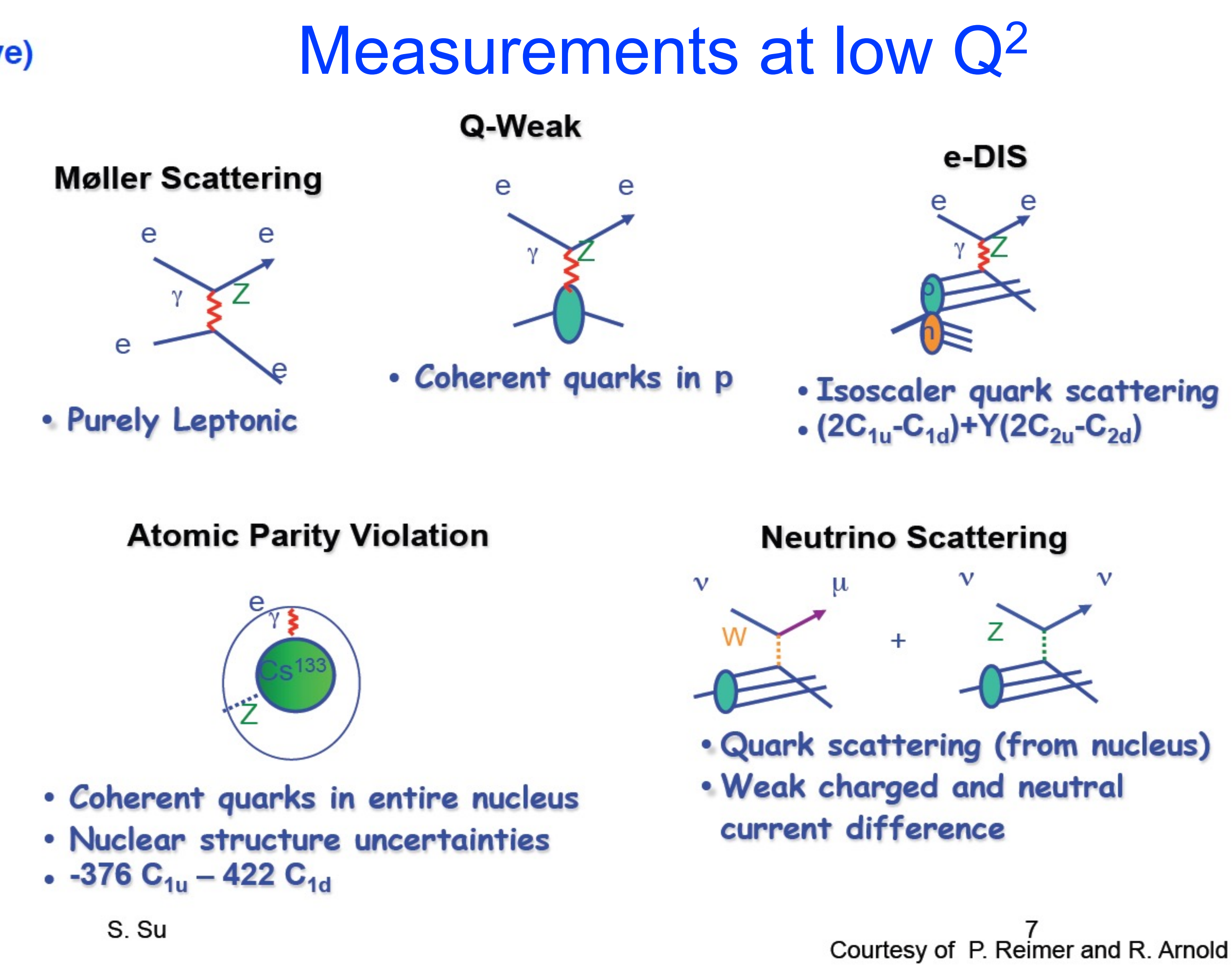

$\sin^2 \theta_W = 0.238$

$\theta_W = 29.2°$

High precision measurements of the Weinberg angle $\sin^2 \theta_W$ at low energy

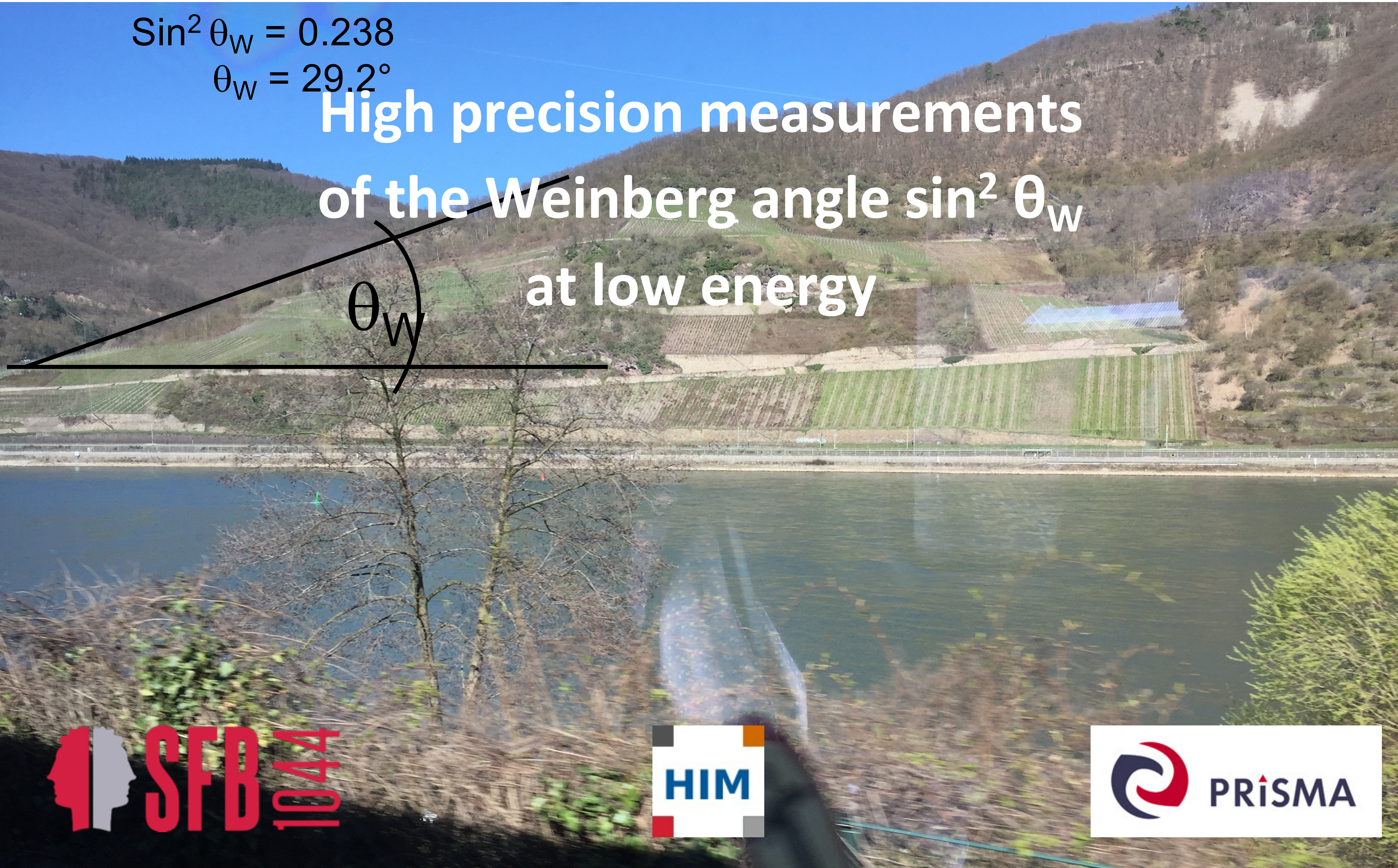

Weak mixing angle $\sin^2 \theta_W$

$\sin^2 \theta_W$: a central parameter of the standard model,
Quantum corrections: sensitivity to physics beyond the standard model

left-right symmetric

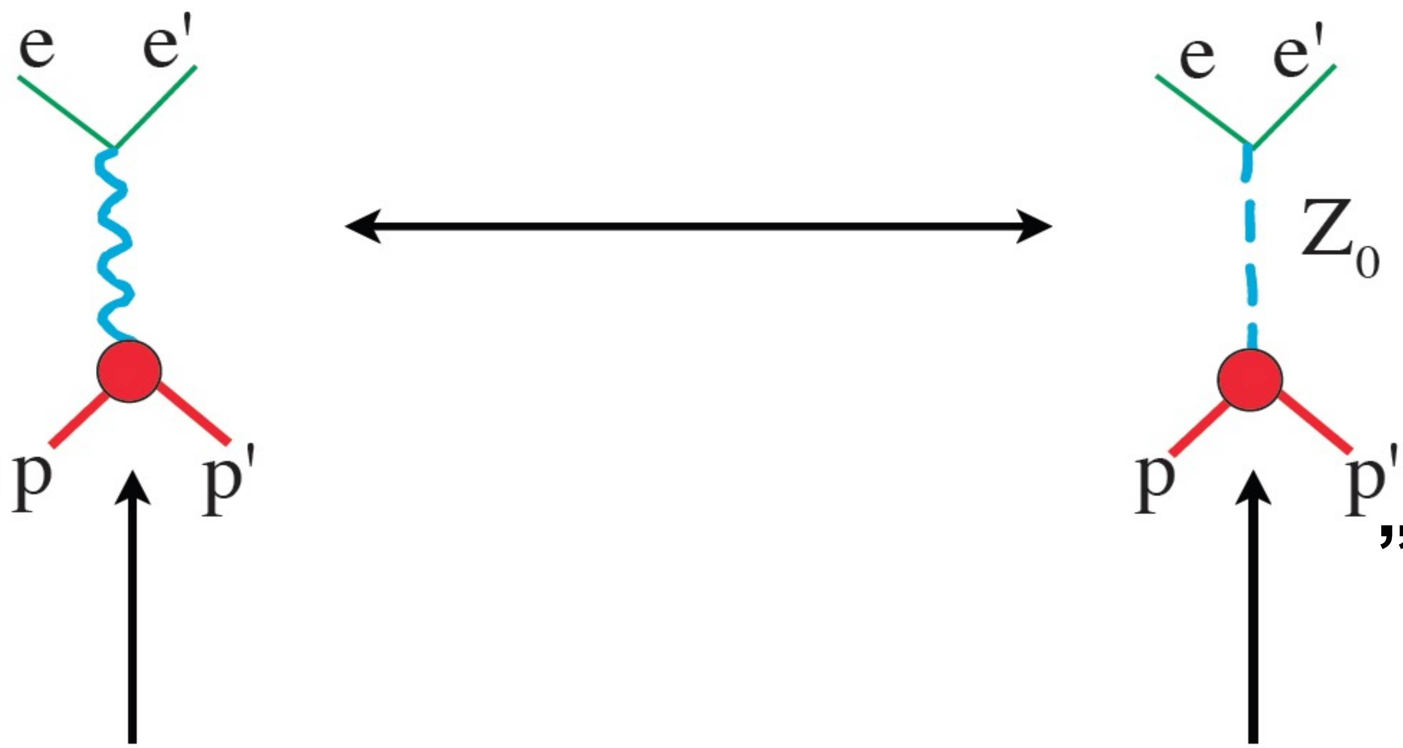

left-right symmetry violated: „parity violation“ measure A_{LR}^{exp}

$Q_e(p) = +1$
electric charge of the proton

$Q_W(p) = 1 - 4 \sin^2 \theta_W = 0.05$
weak charge of the proton
small modification of $\sin^2 \theta_W$: amplified in $Q_W(p)$

This project: A precise determination of $\sin^2 \theta_W$ from parity violating elastic electron proton scattering

Running $\sin^2 \theta_W(\mu)$

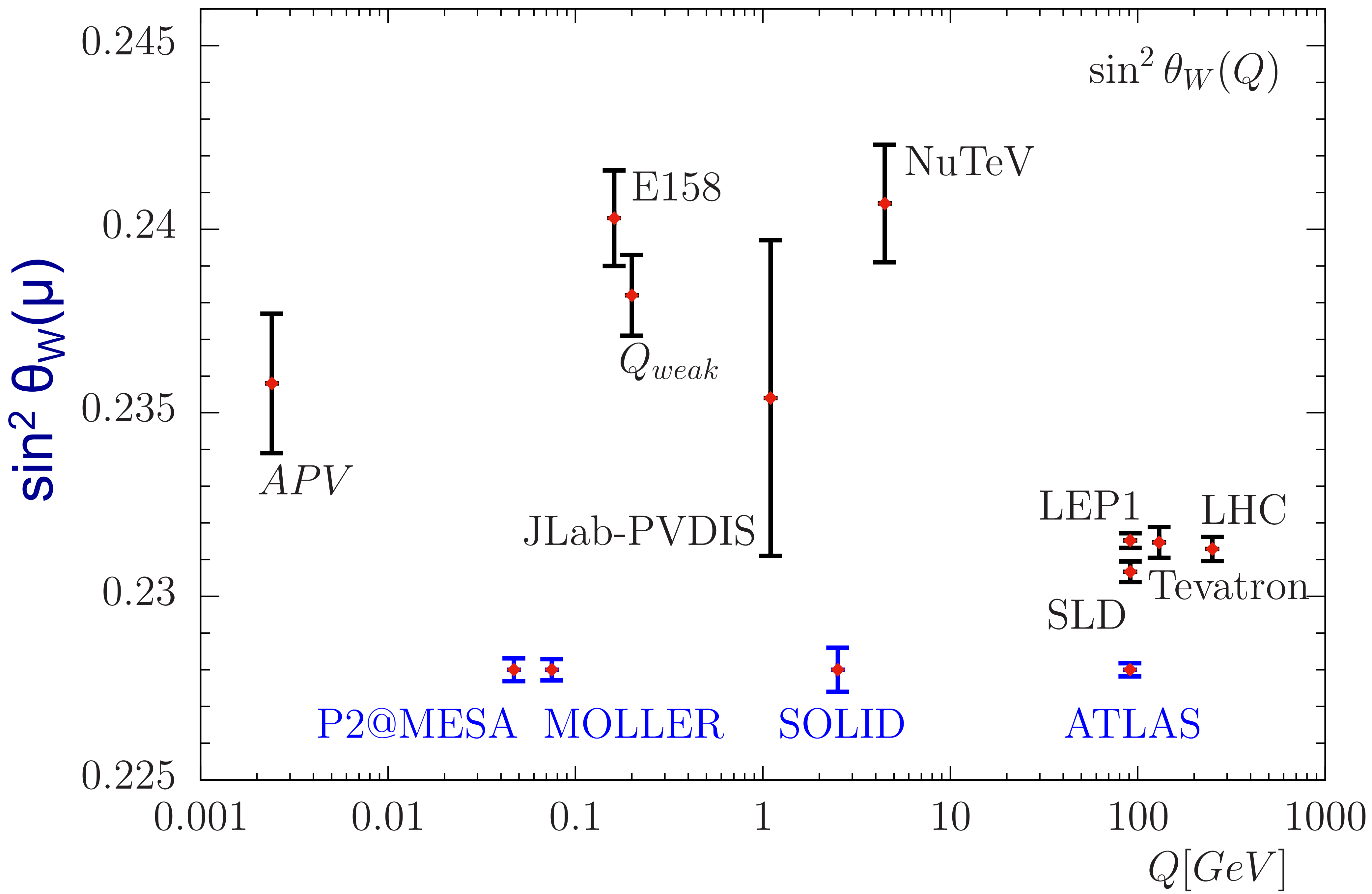

- Process dependent radiative corrections

Running $\sin^2 \theta_W(\mu)$

on Z-pole
$$\left(\frac{\Gamma_Z}{m_Z}\right)^2 = 10^{-3}$$

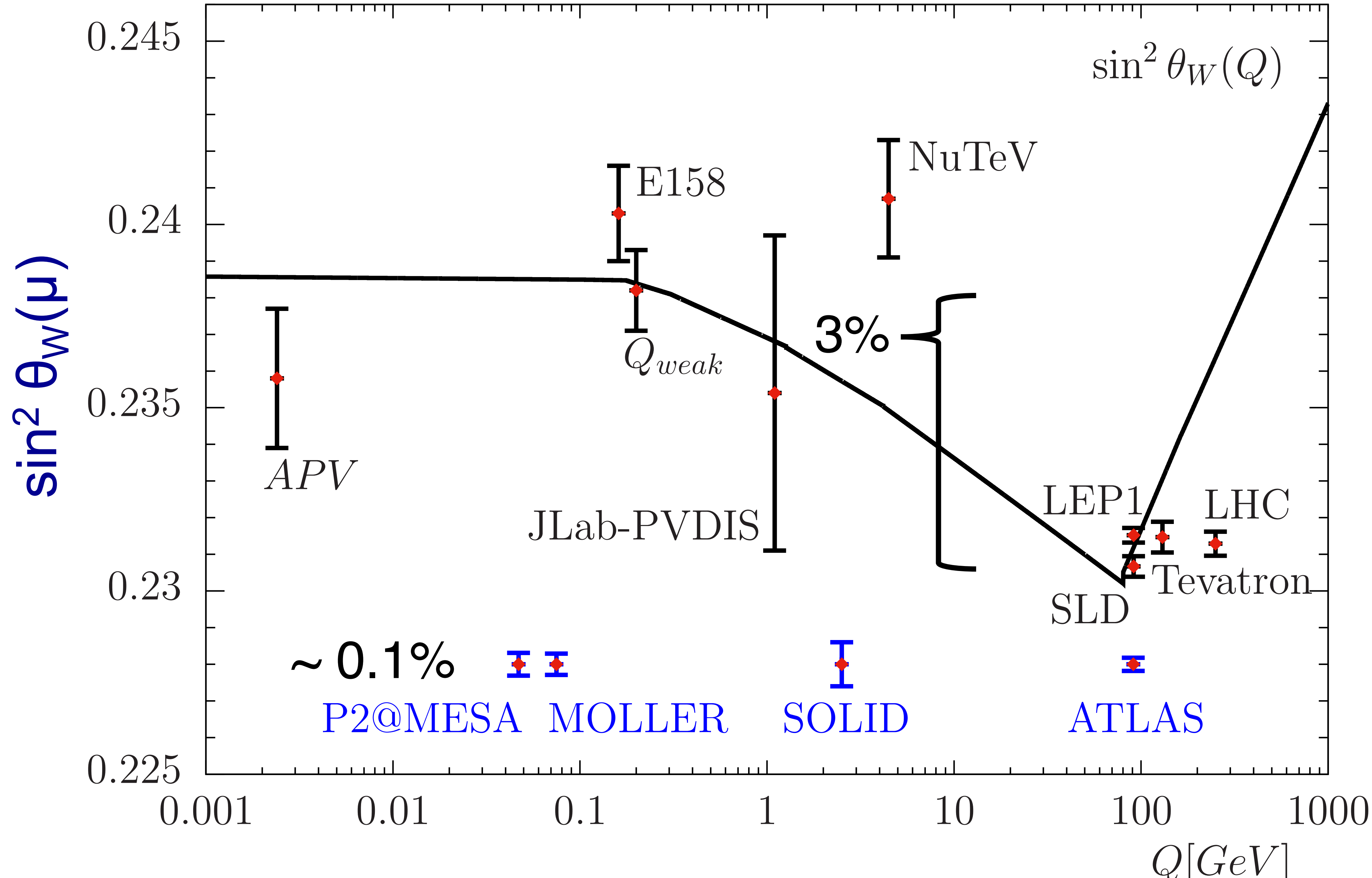

- Sensitive SM-test of the running $\sin^2 \theta_W(\mu)$
- Sensitivity to BSM-physics: radiative corrections to real part
- Theory and Experiment on the same level of accuracy
- Complementary to high energy: on Z-pole real part by 10^{-3} suppressed

Different Portals for SM-extensions

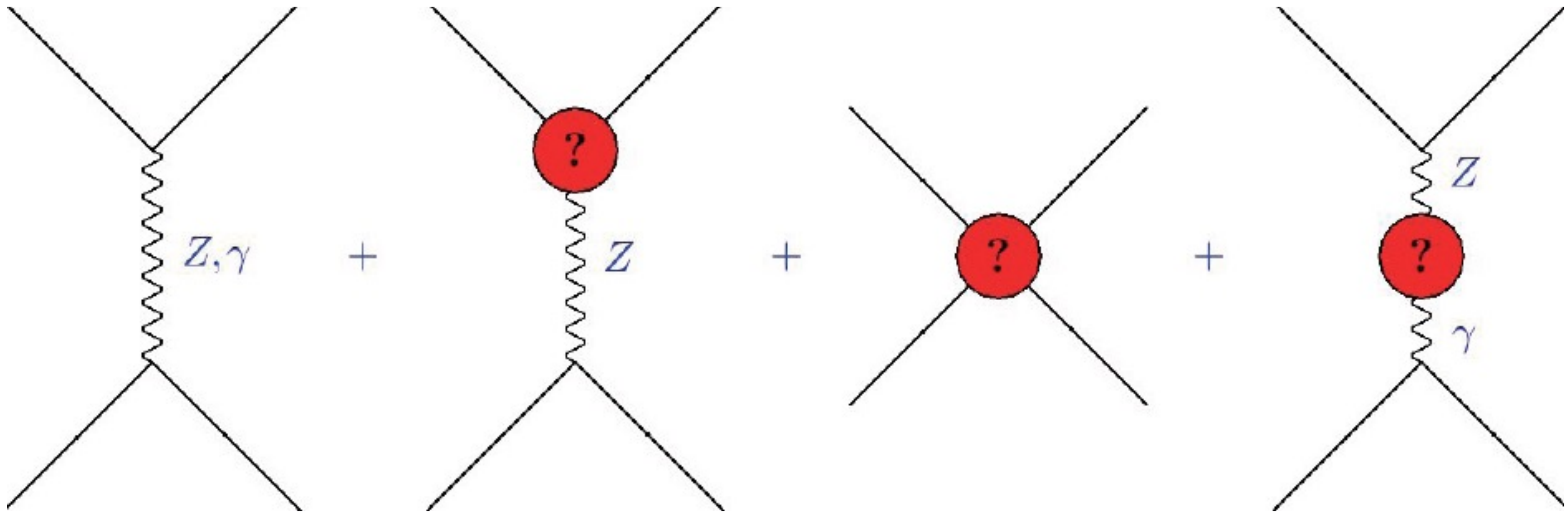

Extra Z

Mixing with Dark photon

Complementary to LHC
Sensitivity to low masses of
$m_{Z'} > 70$ MeV

Contact interaction

Only parameter: Mass of new physics scale
p: 49 TeV
C^{12} + p

New Fermions

R-parity violating SUSY not well constrained from LHC

Running $\sin^2\theta_W$ and Dark Parity Violation

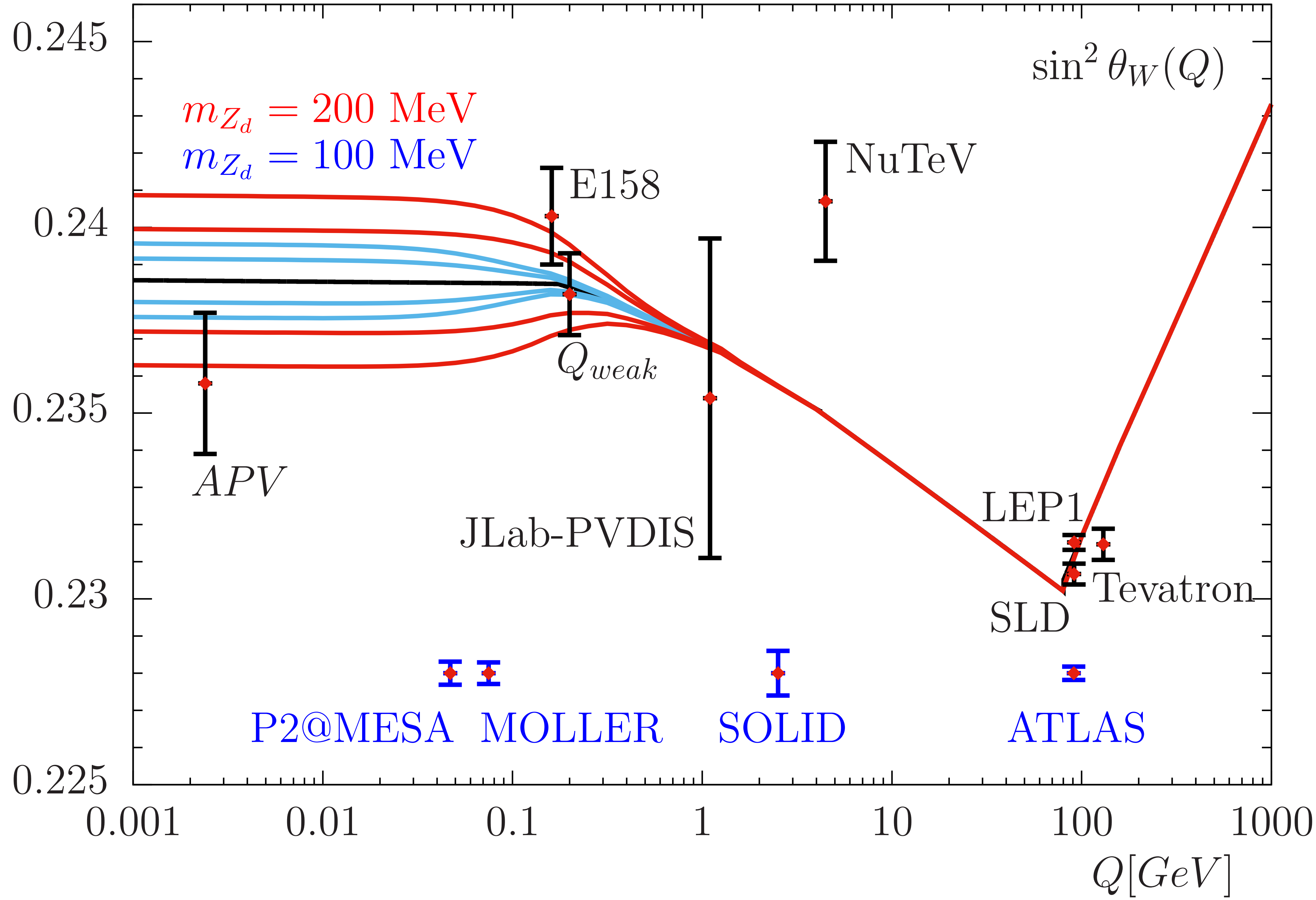

- Large parameter space not excluded from other experiments
- Sensitivity down to masses of 70 MeV

Supersymmetry (RPV)

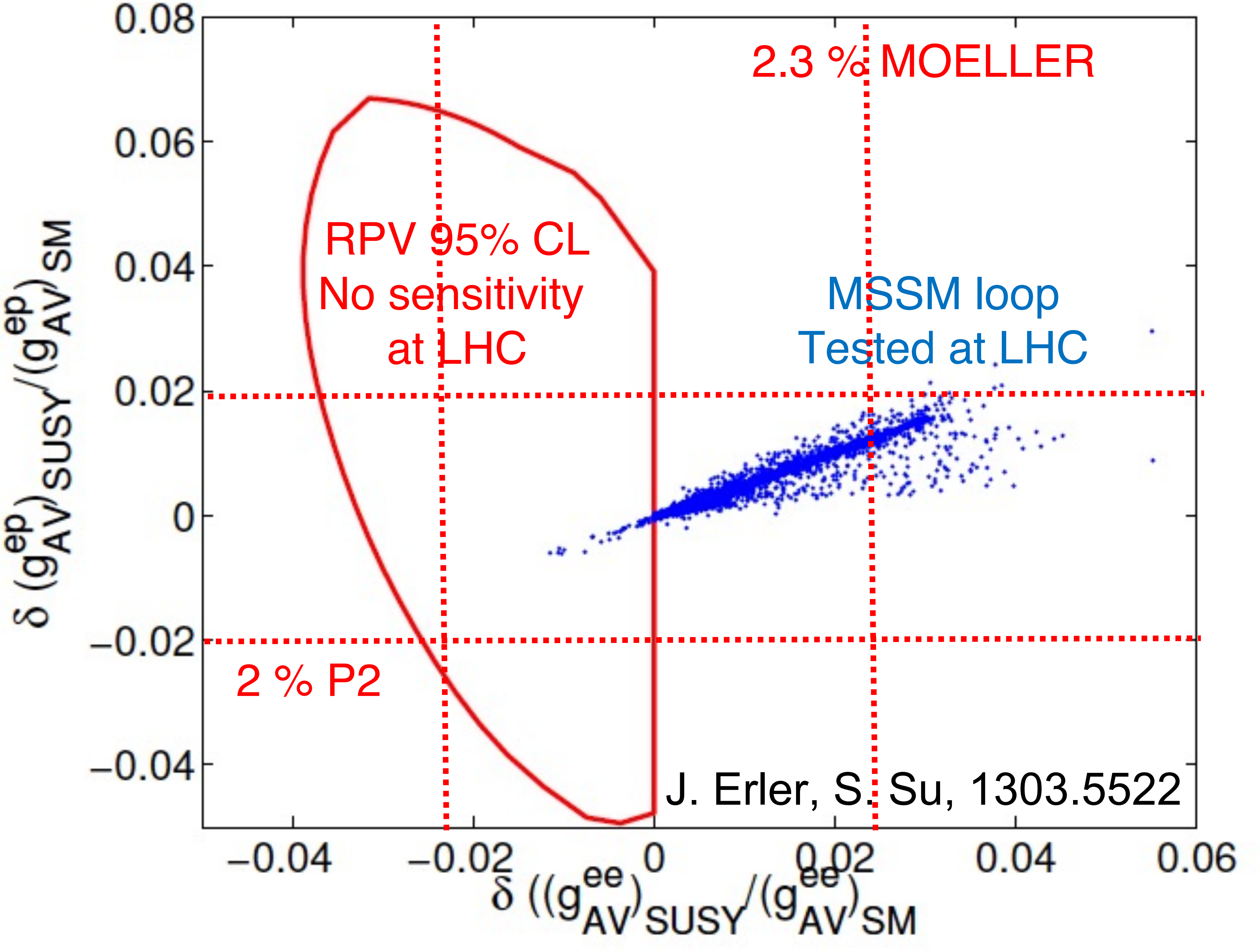

- LHC not very sensitive to RPV SUSY

Contact interaction

	precision	$\Delta \sin^2\overline{\theta}_W(0)$	Λ_{new} (expected)
APV Cs	0.58 %	0.0019	32.3 TeV
E158	14 %	0.0013	17.0 TeV
Qweak I	19 %	0.0030	17.0 TeV
Qweak final	4.5 %	0.0008	33 TeV
PVDIS	4.5 %	0.0050	7.6 TeV
SoLID	0.6 %	0.00057	22 TeV
MOLLER	2.3 %	0.00026	39 TeV
P2	2.0 %	0.00036	49 TeV
PVES ^{12}C	0.3 %	0.0007	49 TeV

70 TeV combined

- Present limits fromLHC: 30 TeV (140 fb^{-1})
- LHC after Run 3, 2024 : 36 TeV (300 fb^{-1})
- LHC after HI-LUMI LHC (2035): 65 TeV (3000 fb^{-1})

Future wEFT constraints from APV and PVES

Adam Falkowski at Mainz MITP workshop: Impact on low energy measurements

Current QWEAK, PVDIS, and APV cesium experiments:

$$\begin{pmatrix} \delta g_{AV}^{eu} \\ \delta g_{AV}^{ed} \\ 2\delta g_{VA}^{eu} - \delta g_{VA}^{ed} \end{pmatrix} = \begin{pmatrix} 0.74 \pm 2.2 \\ -2.1 \pm 2.5 \\ -39 \pm 54 \end{pmatrix} \times 10^{-3}$$

Projections from combined P2, SoLID, and APV radium experiments:

$$\begin{pmatrix} \delta g_{AV}^{eu} \\ \delta g_{AV}^{ed} \\ 2\delta g_{VA}^{eu} - \delta g_{VA}^{ed} \end{pmatrix} = \begin{pmatrix} 0 \pm 0.70 \\ 0 \pm 0.97 \\ 0 \pm 7.4 \end{pmatrix} \times 10^{-3}$$

$$\mathcal{L}_{\mathrm{wEFT}} \supset -\frac{1}{2v^2} \sum_{q=u,d} g_{AV}^{eq} (\bar{e}\,\bar{\sigma}_\rho e - e^c \sigma_\rho \bar{e}^c)(\bar{q}\,\bar{\sigma}^\rho q + q^c \sigma^\rho \bar{q}^c)$$
$$-\frac{1}{2v^2} \sum_{q=u,d} g_{VA}^{eq} (\bar{e}\,\bar{\sigma}_\rho e + e^c \sigma_\rho \bar{e}^c)(\bar{q}\,\bar{\sigma}^\rho q - q^c \sigma^\rho \bar{q}^c)$$

AA, Grilli Di Cortona, Tabrizi 1802.08296

AA, Gonzalez-Alonso in progress

Constraints from PVES at MESA

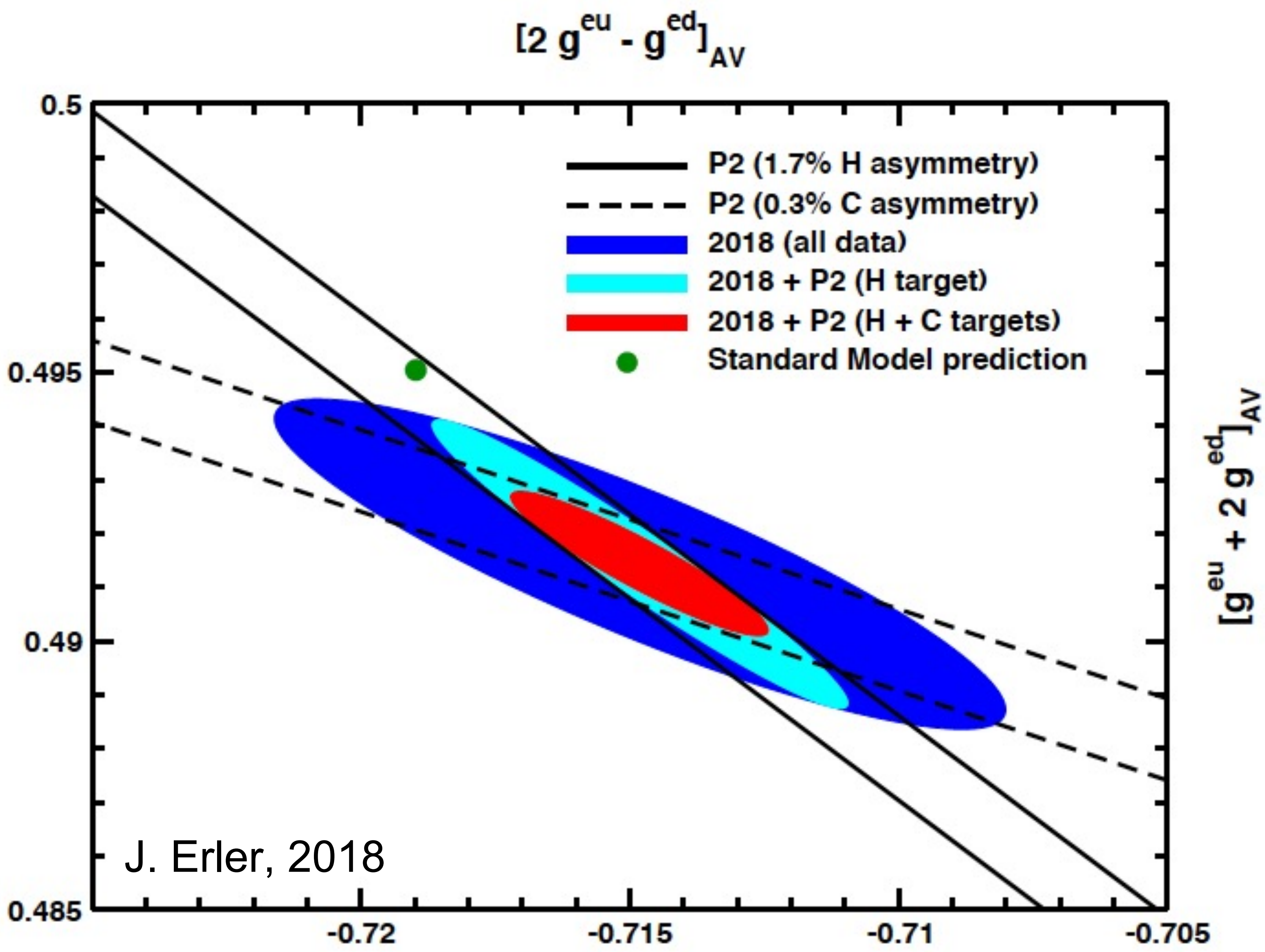

- Quark-vector-electron-axial vector couplings
- Sensitivity down to masses of 70 MeV and up to masses of 70 TeV

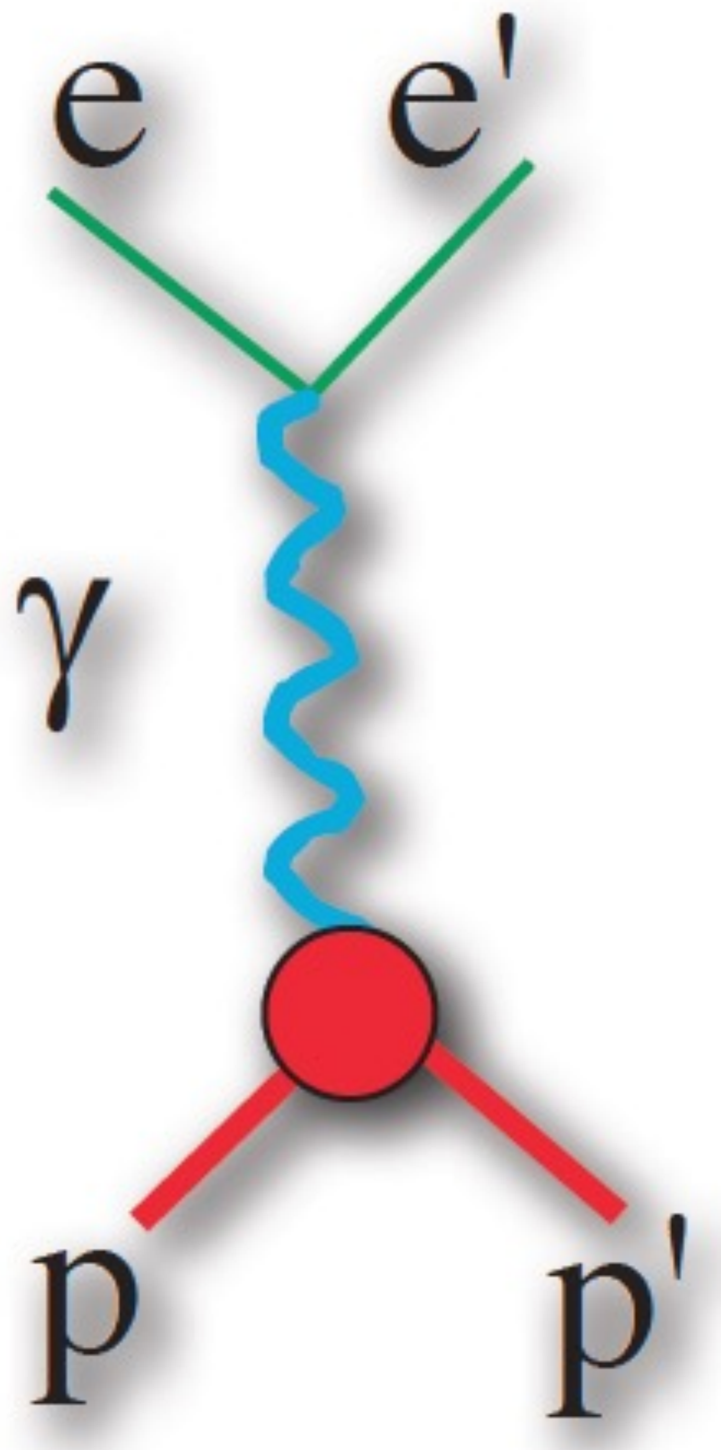

$$\sigma \sim \mathcal{M}\,\mathcal{M}^{*}\ \text{Phasespace}$$

$$\sim \left(j_\mu \frac{1}{Q^2} J^\mu\right)\left(j_\mu \frac{1}{Q^2} J^\mu\right)^{*}$$

$$j_\mu \sim \bar{e}\,\gamma_\mu\, e \ \ \text{Vector Current}$$

$$J^\mu_\gamma \sim \left\langle N \middle| q^u \bar{u}\,\gamma_\mu\, u + q^d \bar{d}\,\gamma_\mu d + q^s \bar{s}\,\gamma_\mu s \middle| N' \right\rangle$$

$$= \bar{\mathcal{P}}\left[\gamma^\mu F_1 - i\sigma^{\mu\nu} q_\nu \frac{\kappa_p}{2M_N} F_2\right]\mathcal{P}$$

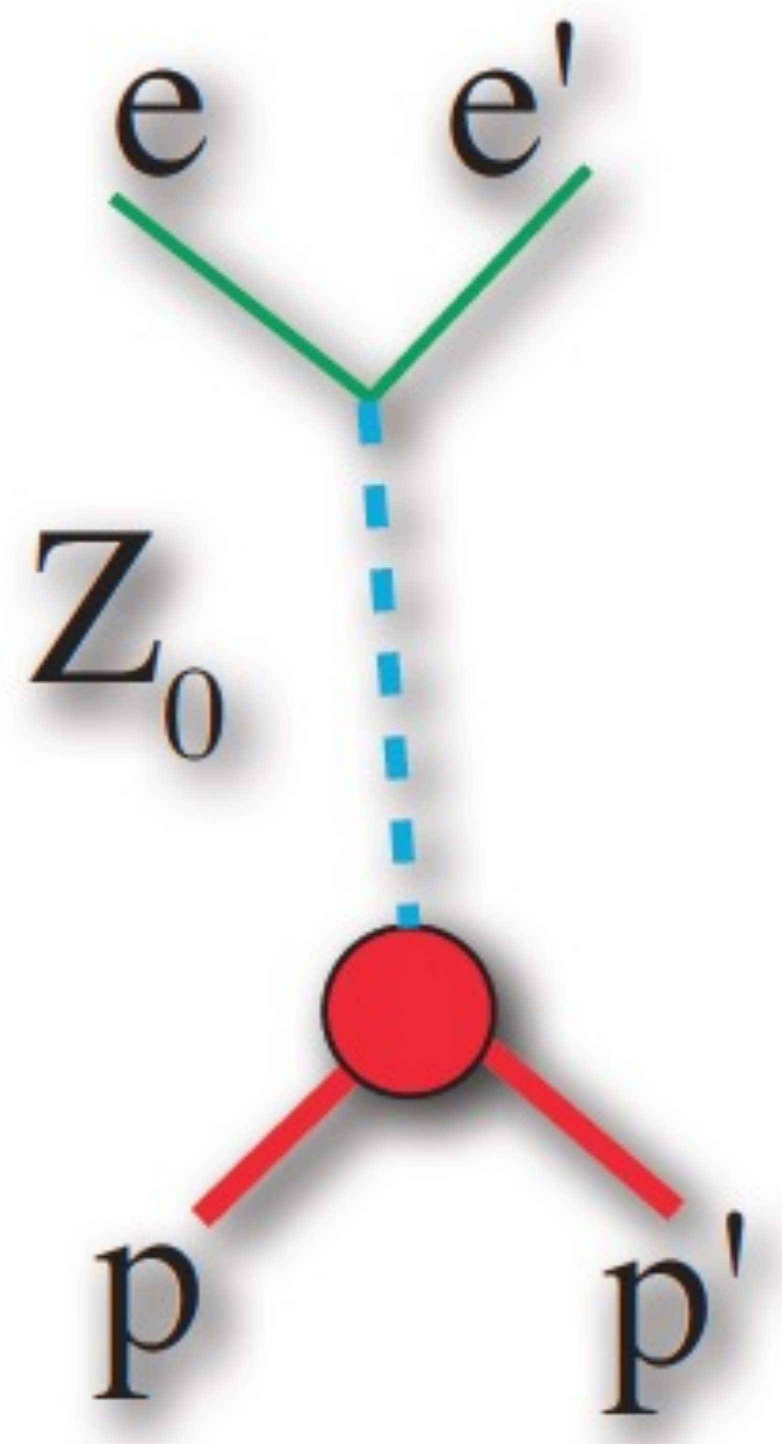

$$\tilde{q}^{d}{}_{V} = \tau_3 - 2q^{d} \sin^2(\theta_W)$$

$$\begin{aligned} \tilde{J}^{\mu}_{Z} &\sim \left\langle N \middle| \tilde{q}^{u}\,\overline{u}\,\gamma_\mu\, u + \tilde{q}^{d}\,\overline{d}\,\gamma_\mu d + \tilde{q}^{s}\,\overline{s}\,\gamma_\mu s \middle| N' \right\rangle \\ &= \overline{\mathcal{P}}\left[\gamma^{\mu}\tilde{F}_1 - i\sigma^{\mu\nu} q_\nu \frac{\kappa_p}{2M_N}\tilde{F}_2\right]\mathcal{P} \end{aligned}$$

ing Asymmetry in elastic electron proton scattering

$\sigma \approx$

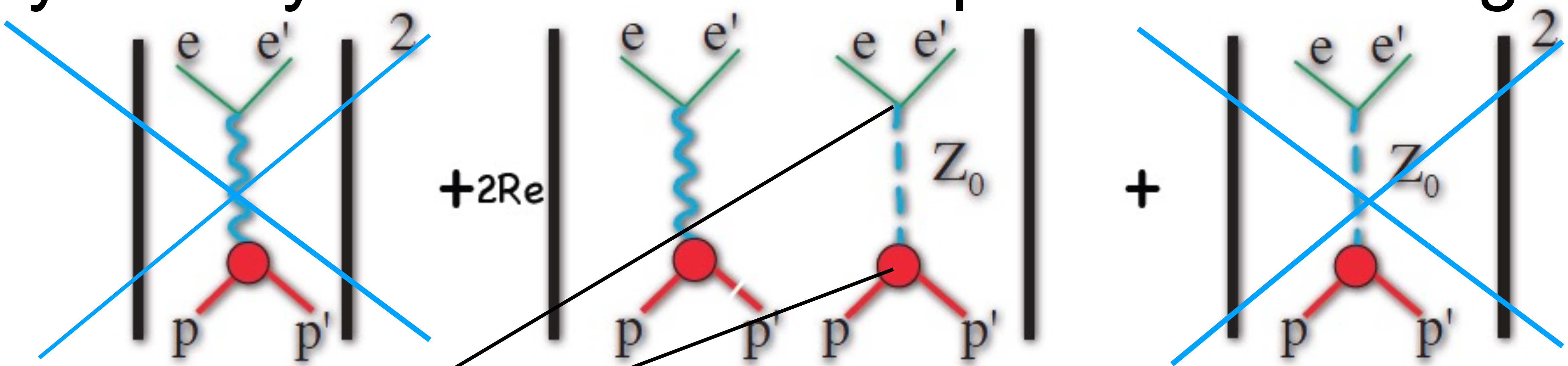

V-A coupling:
parity-violating
cross section asymmetry A_{LR}
longitudinally pol. electrons
unpolarised protons

$$(V\text{-}A)_e(V\text{-}A)_p$$
$$A_eV_p+V_eA_p$$

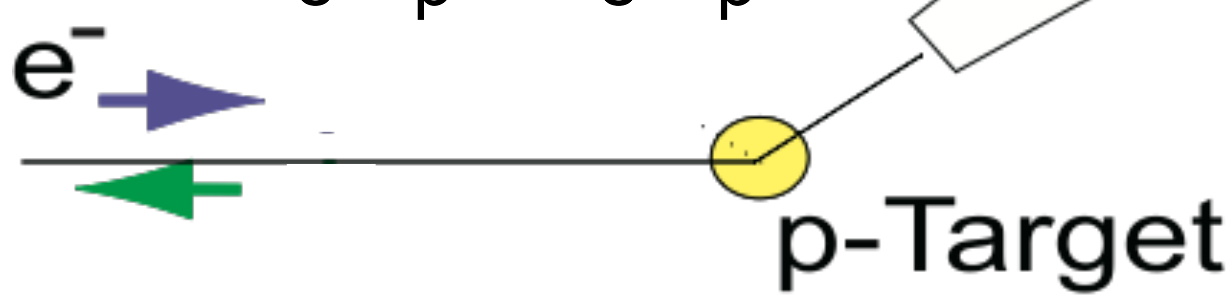

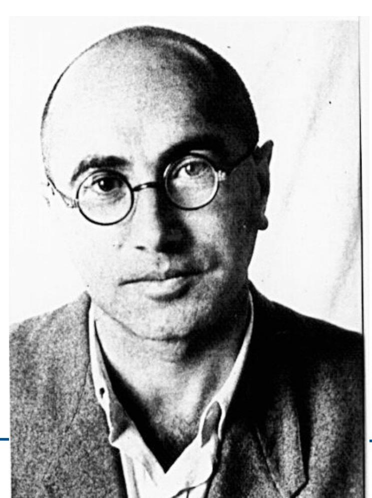

LETTERS TO THE EDITOR

PARITY NONCONSERVATION IN THE FIRST ORDER IN THE WEAK-INTERACTION CONSTANT IN ELECTRON SCATTERING AND OTHER EFFECTS

Ya. B. ZEL' DOVICH

Submitted to JETP editor December 25, 1958

J. Exptl. Theoret. Phys. (U.S.S.R.) 36, 964-966

Das Bildelement mit der Beziehungs-ID rId51 wurde in der Datei nicht gefunden.

Parity violating cross section asymmetry

weak charge

$$A_{LR} = \frac{\sigma(e\uparrow) - \sigma(e\downarrow)}{\sigma(e\uparrow) + \sigma(e\downarrow)} = -\frac{G_F Q^2}{4\sqrt{2}\pi\alpha}\left(Q_W - F(Q^2)\right)$$

$$Q_W = 1 - 4\sin^2\theta_W(\mu)$$

hadron structure

$$F(Q^2) = F_{EM}(Q^2) + F_{Axial}(Q^2) + F_{Strange}(Q^2)$$

Sensitivity to new physics up to 50 TeV

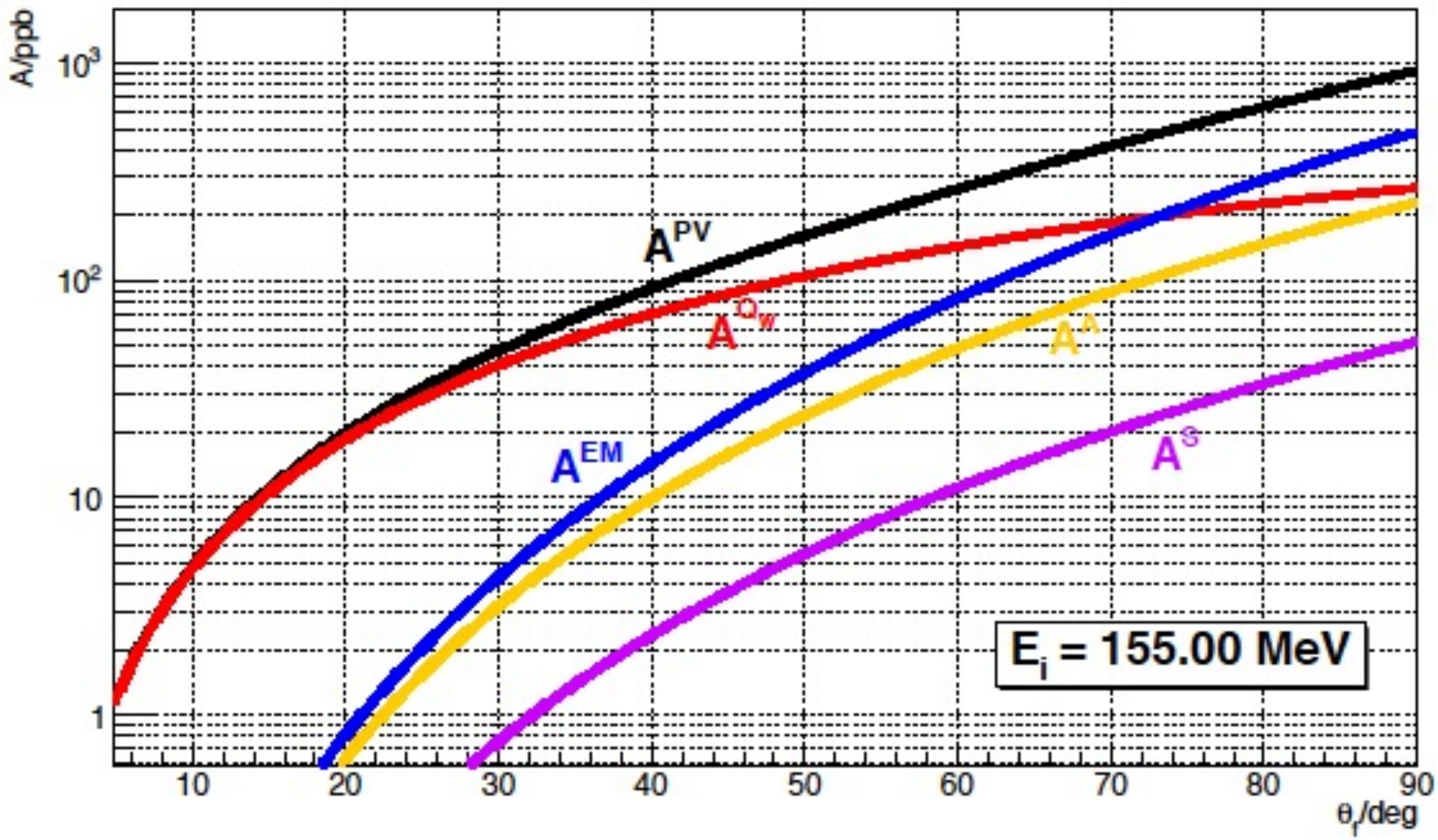

Projected Experiment Sensitivity

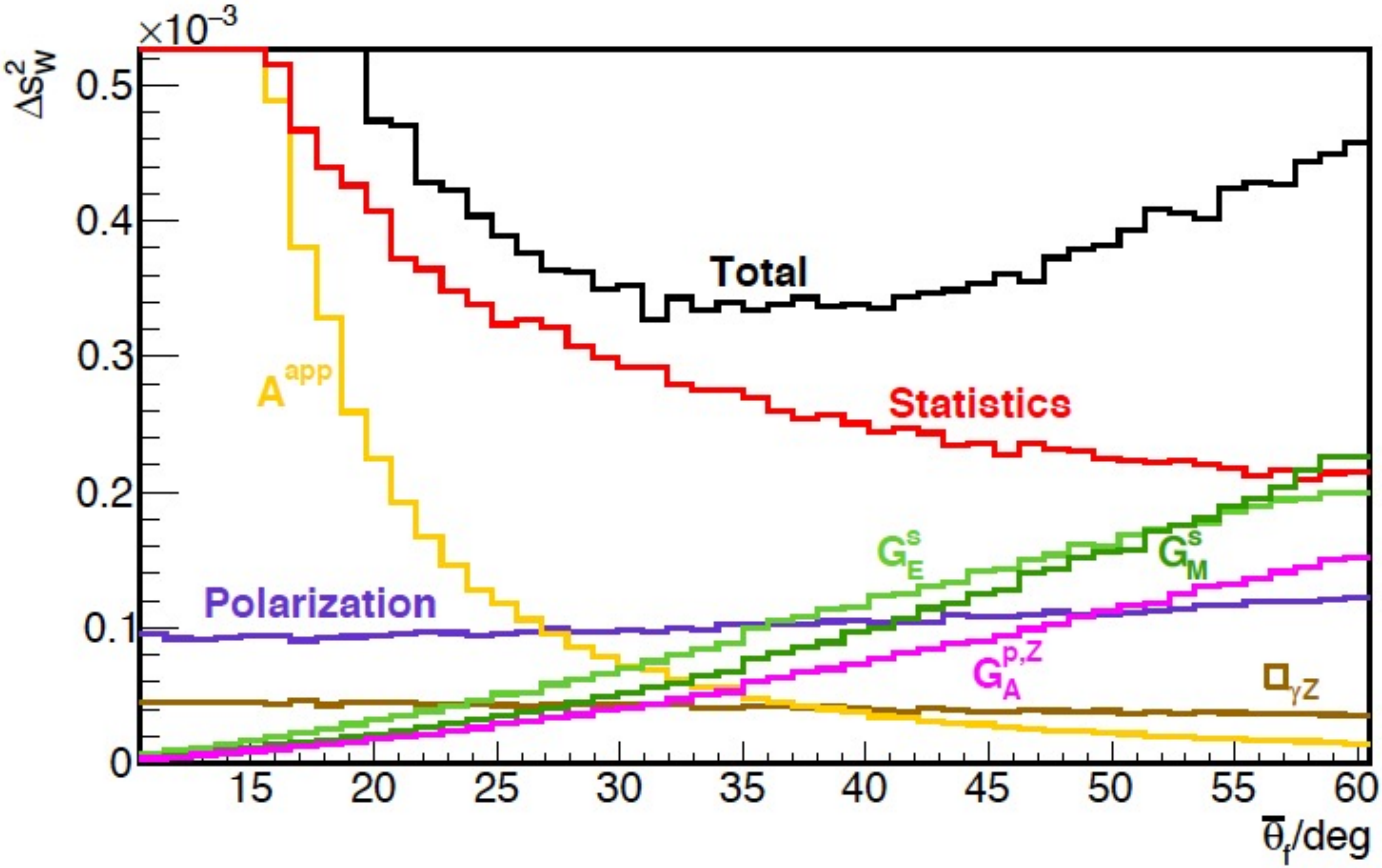

Achievable precision in $\sin^2\Theta_W$

P2 Experiment conditions

E_{beam}	155 MeV
$\bar{\theta}_{\text{f}}$	35°
$\delta\theta_{\text{f}}$	20°
s^2_{W}	0.231 16
$\Delta_{\text{exp}} s^2_{\text{W}}$	3.7×10^{-4} (0.16 %)
$\Delta_{\text{exp, stat}} s^2_{\text{W}}$	3.1×10^{-4} (0.13 %)
$\Delta_{\text{exp, P}} s^2_{\text{W}}$	0.7×10^{-4} (0.03 %)
$\Delta_{\text{exp, false}} s^2_{\text{W}}$	0.6×10^{-4} (0.03 %)
$\Delta_{\text{exp, t.w.}} s^2_{\text{W}}$	1.2×10^{-4} (0.05 %)
$\Delta_{\text{exp, t.p.}} s^2_{\text{W}}$	0.1×10^{-4} (0.00 %)
$\Delta_{\text{exp},\Box_{\gamma Z}} s^2_{\text{W}}$	0.4×10^{-4} (0.02 %)
$\Delta_{\text{exp, nucl. FF}} s^2_{\text{W}}$	1.2×10^{-4} (0.05 %)

Impact including ^{12}C

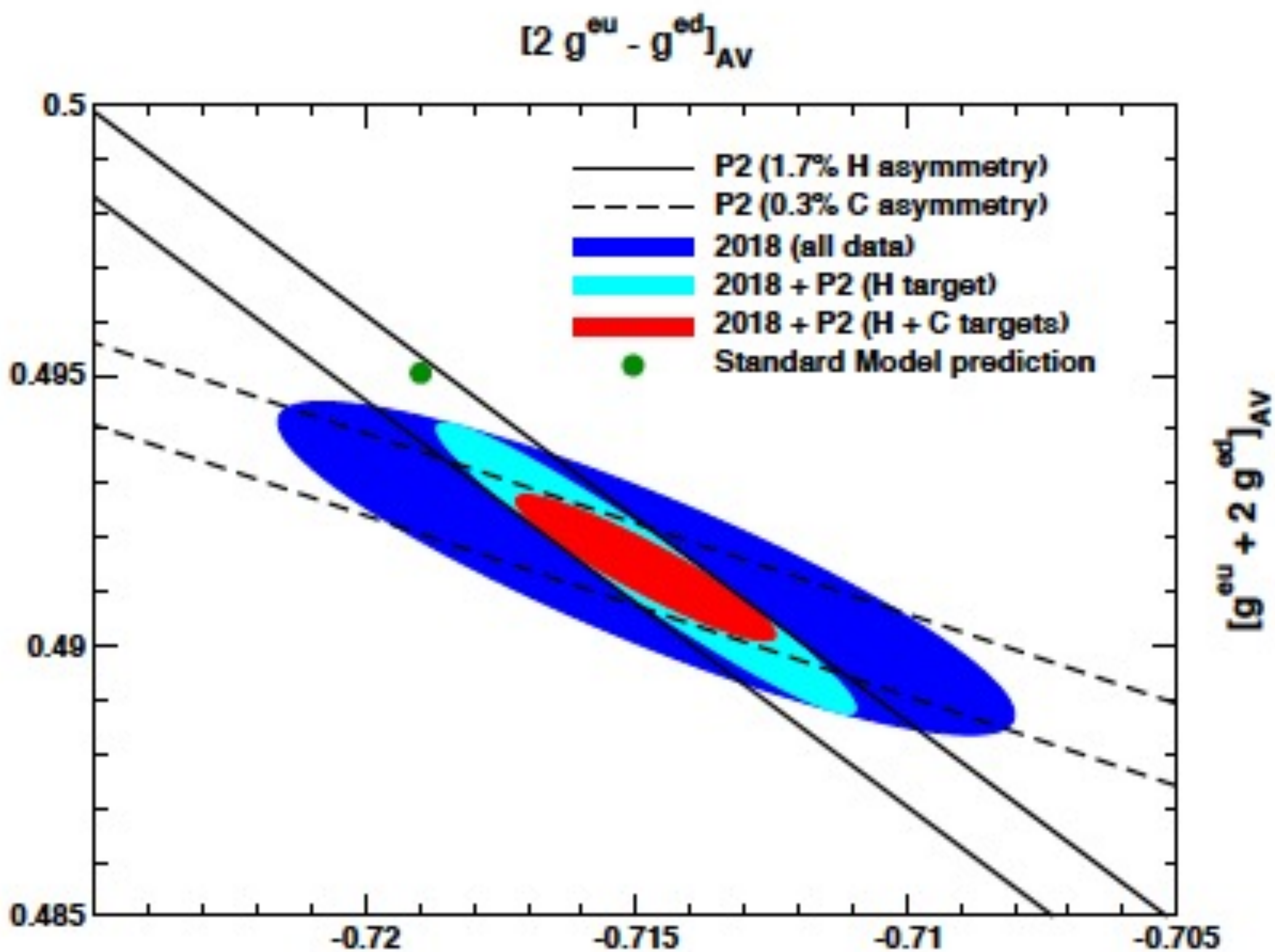

Kohlenstoff

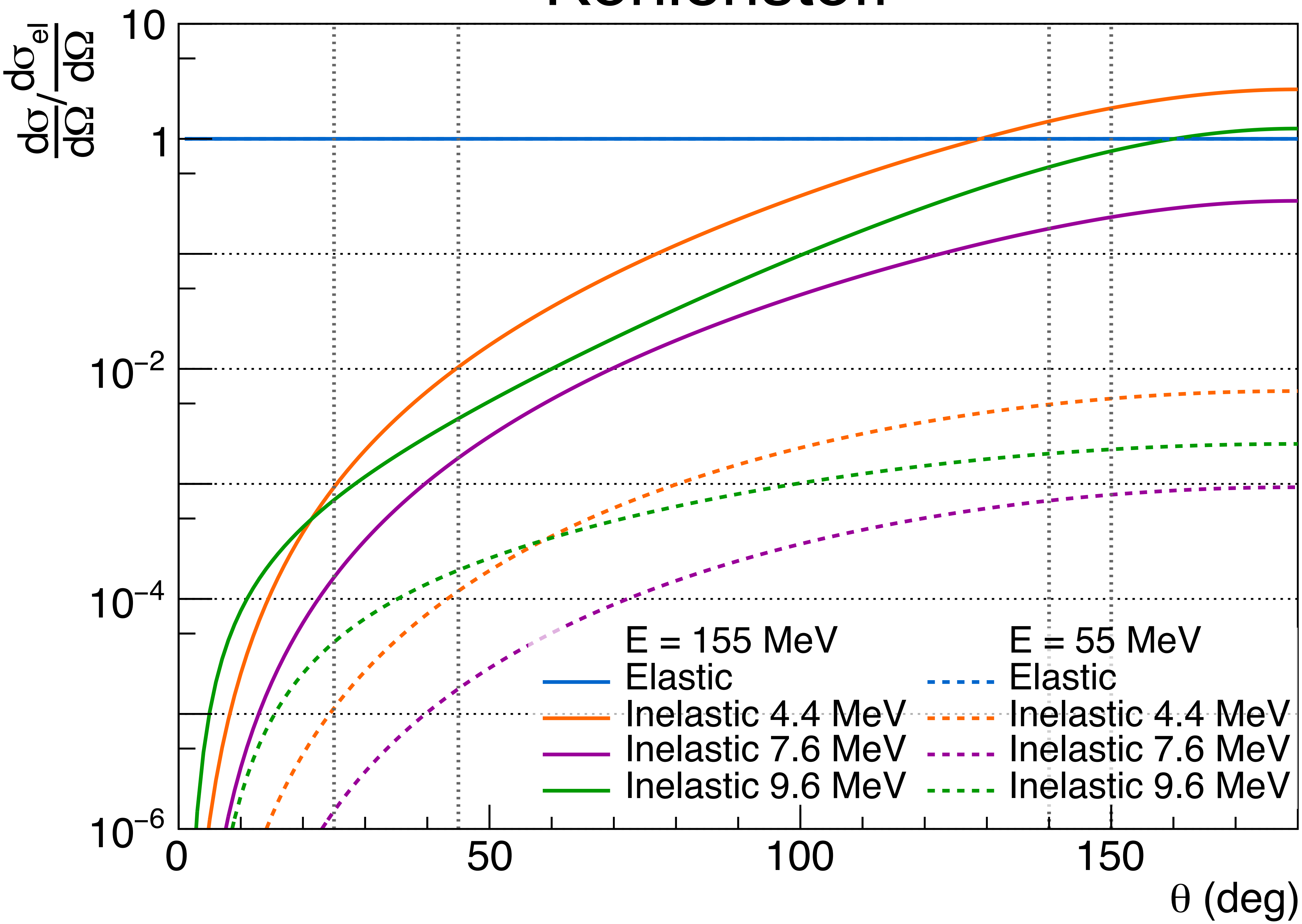

Target	Wasserstoff					
Winkelbereich	Vorwärts 25°-45°					
Strahlenergie	55 MeV		55 MeV		155 MeV	
Strahlstrom	20 µA		150 µA		150 µA	
Asymmetrie <A>	-2.8 ppb		-2.8 ppb		-28.1 ppb	
Virtualität <Q²>	$4.7\ 10^{-4}$ GeV²/c²		$4.7\ 10^{-4}$ GeV²/c²		$4.8\ 10^{-3}$ GeV²/c²	
Rate (alle Teilchen)	572 GHz		4 287 GHz		1 439 GHz	
Rate (Primäre Elektronen)	111 GHz		833 GHz		109 GHz	
Messzeit	100 h	10 000 h	100 h	10 000 h	100 h	10 000 h
Gesamt Fehler ΔA	4.9 ppb (181%)	0.49 ppb (17.4%)	1.7 ppb (62%)	0.21 ppb (7.6%)	5.0 ppb (17,7%)	0.6 ppb (2.2%)
Statistische Fehler ΔA	4.7 ppb (172%)	0.48 ppb (17.3%)	1.7 ppb (62%)	0.17 ppb (6.2%)	4.9 ppb (17.2%)	0.5 ppb (1.8%)
Gesamt Fehler $\Delta\sin^2\theta_W$	10,8%	1,1%	3,8%	0,5%	1,1%	0,14%
Statistische Fehler $\Delta\sin^2\theta_W/\sin^2\theta_W$	10,5%	1,1%	3,8%	0,4%	1,1%	0,13%

Target					
Winkelbereich		Rückwärts 140°-150°			
Strahlenergie		55 MeV		155 MeV	
Strahlstrom		150 µA		150 µA	
Asymmetrie <A>		-0.2 ppm		-4.6 ppm	
Virtualität <Q²>		$6\ 10^{-3}$ GeV²/c²		$6.7\ 10^{-2}$ GeV²/c²	
Rate (alle Teilchen)		13 888 GHz		10 314 GHz	
Rate (Primäre Elektronen)		0.75 GHz		0.11 GHz	
Messzeit		100 h	1 000 h	100 h	1 000 h
Gesamt Fehler ΔA	4)				
Statistische Fehler ΔA	4)		10,9%		1,4%
Gesamt Fehler $\Delta\sin^2\theta_W$					
Statistische Fehler $\Delta\sin^2\theta_W/\sin^2\theta_W$					

Target	Kohlenstoff							
Winkelbereich	Vorwärts 25°-45°							
Strahlenergie	55 MeV		55 MeV		155 MeV		155 MeV	
Strahlstrom	7.5 µA		150 µA		75 µA		150 µA	
Asymmetrie <A>	47.9 ppb		47.9 ppb		416.3 ppb		416.3 ppb	
Virtualität <Q²>	$5.8\ 10^{-4}$ GeV²/c²		$5.8\ 10^{-4}$ GeV²/c²		$5.0\ 10^{-3}$ GeV²/c²		$5.0\ 10^{-3}$ GeV²/c²	
Rate (alle Teilchen)	436 GHz		8 730 GHz		958 GHz		1 916 GHz	
Rate (Primäre Elektronen)	121 GHz		2 421 GHz		125 GHz		249 GHz	
Messzeit	100 h	2 500 h	100 h	2 500 h	100 h	2 500 h	100 h	2 500 h
Gesamt Fehler ΔA	4.6 ppb (9.6%)	0.94 ppb (2.0%)	1.1 ppb (2.2%)	0.3 ppb (0.7%)	5.1 ppb (1.2%)	2.3 ppb (0.5%)	3.7 ppb (0.9%)	2.2 ppb (0.5%)
Statistische Fehler ΔA	4.5 ppb (9.4%)	0.90 ppb (1.9%)	1.0 ppb (2.1%)	0.2 ppb (0.4%)	4.6 ppb (1.1%)	0.9 ppb (0.2%)	3.3 ppb (0.8%)	0.7 ppb (0.2%)
Gesamt Fehler $\Delta\sin^2\theta_W$	9,6%	2,0%	2,2%	0,7%	1,2%	0,5%	0,9%	0,5%
Statistische Fehler $\Delta\sin^2\theta_W/\sin^2\theta_W$	9,4%	1,9%	2,1%	0,4%	1,1%	0,2%	0,8%	0,2%

Target				
Winkelbereich	Rückwärts 140°-150°			
Strahlenergie	55 MeV		155 MeV	
Strahlstrom	150 µA		150 µA	
Asymmetrie <A>	0.76 ppm		6.6 ppm	
Virtualität <Q²>	$9.1\ 10^{-3}$ GeV²/c²		$7.97\ 10^{-2}$ GeV²/c²	
Rate (alle Teilchen)				
Rate (Primäre Elektronen)	0.74 GHz		1.2 MHz	
Messzeit	100 h	1 000 h	100 h	1 000 h
Gesamt Fehler ΔA				
Statistische Fehler ΔA	8,0%	2,5%	22,9%	7,2%
Gesamt Fehler $\Delta\sin^2\theta_W$				
Statistische Fehler $\Delta\sin^2\theta_W/\sin^2\theta_W$	8,0%	2,5%	22,9%	7,2%

Qweak@Jlab	P2@MESA hydrogen	P2@MESA carbon	P2@MESA lead
A_{ep}=-226.5 ppb	A_{ep}=-28 ppb	A_{ep}= 416.3 ppb	See talk by Michaela Thiel
ΔA_{ep}= 9.3 ppb	ΔA_{ep}= 0.5 ppb ppb=1/√N Factor 19 After 10,000 h	ΔA_{ep}^{stat}= 2.7 ppb after 300 h ΔA_{ep}^{stat}= 0.9 ppb after 2500 h	
$\Delta A_{ep}/A_{ep}$= 4.2 %	$\Delta A_{ep}/A_{ep}$= 1.8 %	$\Delta A_{ep}/A_{ep}^{stat}$= 0.6 % (0.2 %) Polarimetry!	
$\Delta \sin^2 \theta_W / \sin^2 \theta_W$= 0.46 %	$\Delta \sin^2 \theta_W / \sin^2 \theta_W$= 0.15 %	$\Delta \sin^2 \theta_W / \sin^2 \theta_W$= 0.6 %	
	Auxiliary measurements backward angle	Auxiliary measurements backward angle	

Improvement by high luminosity, long measurement time, small systematics, lower Q^2

Experimental method

Parity violating electron scattering

PVeS Experiment Summary

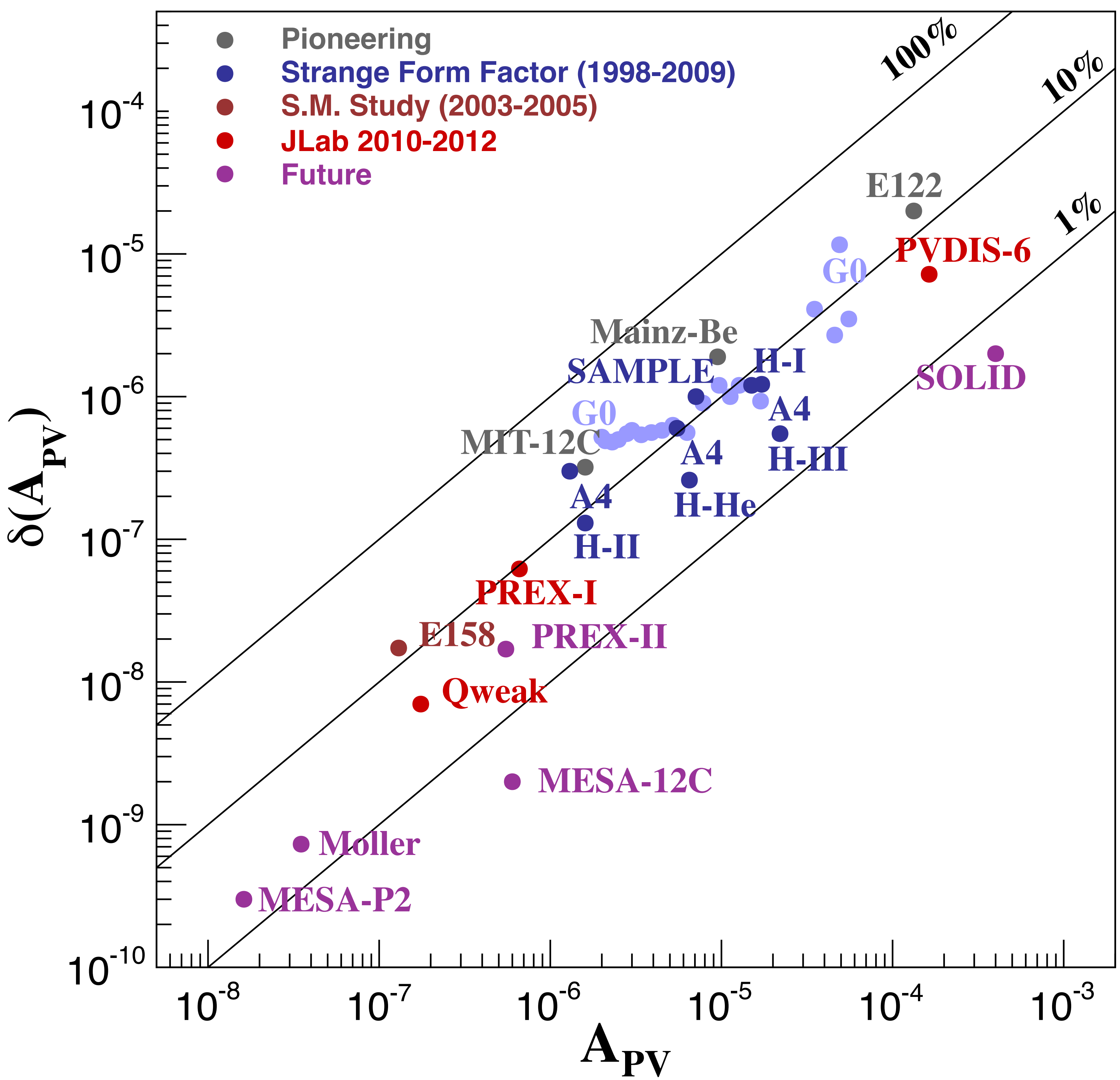

- P2: Challenging experiment
- New concepts on all aspects of experiment
- Factor 3 improved accuracy compared to Jlab Qweak

- Large solid angle magnetic spectrometer: Solenoid
- Integrating detectors for ~100 GHz signal rate
- Polarimetry: $\Delta P = 0.3$ - 0.5%, 3 different polarimeters, double scattering Mott, Hydro-Möller
- 150 μA beam current
- High power target
- Fast digitization of signals
- All solid state tracking for Q^2-measurement: HVmaps
- Existing accelerator MAMI availbale for in situ prototype-tests of all components

Parity violating electron scattering
New developments

False asymmetries
Control of accelerator

$$A_{LR}^{exp} = \frac{\sigma(\vec{e}p)-\sigma(\overleftarrow{e}p)}{\sigma(\vec{e}p)+\sigma(\overleftarrow{e}p)} = -P\,\frac{G_F Q^2}{4\sqrt{2}\pi\alpha}\left(\underbrace{Q_W(p) - F(Q^2)}\right) + A_F$$

Cross section asymmetry A_{LR}^{exp}

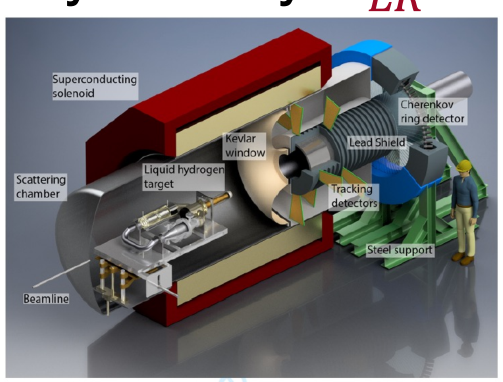

Magnetic spectrometer
Cherenkov detector
Read-out electronics
Data acquisition

Beam polarisation P
Polarimetry

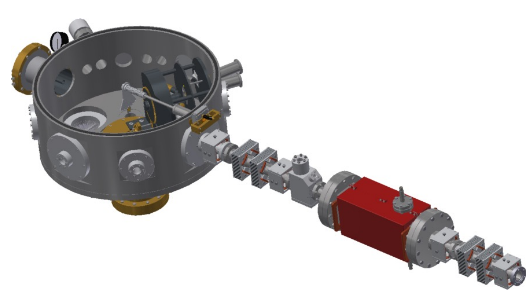

Momentum transfer Q^2
Tracking system

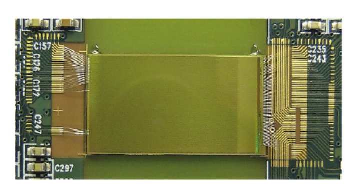

Theory:
QED corrections
EW corrections (two loop)
Hadron structure $F(Q^2)$,
Strangeness form factors
Axial form factor

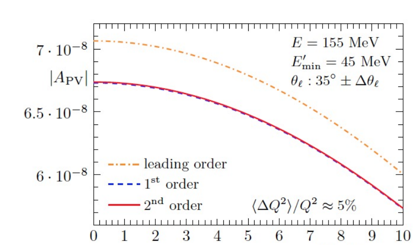

MESA accelerator floorplan

Two operational modes: extracted beam (P2) and energy recovering (MAGIX)

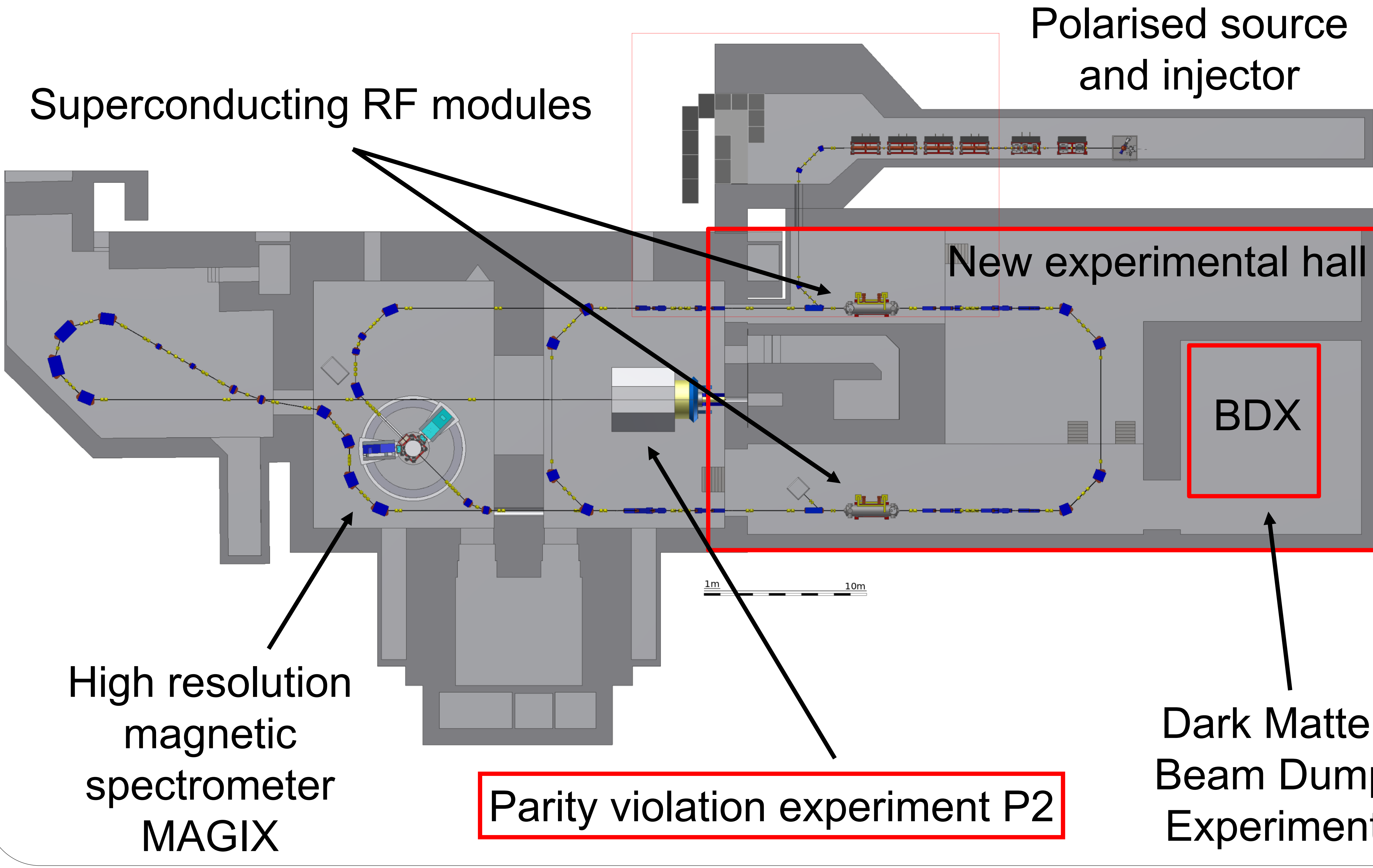

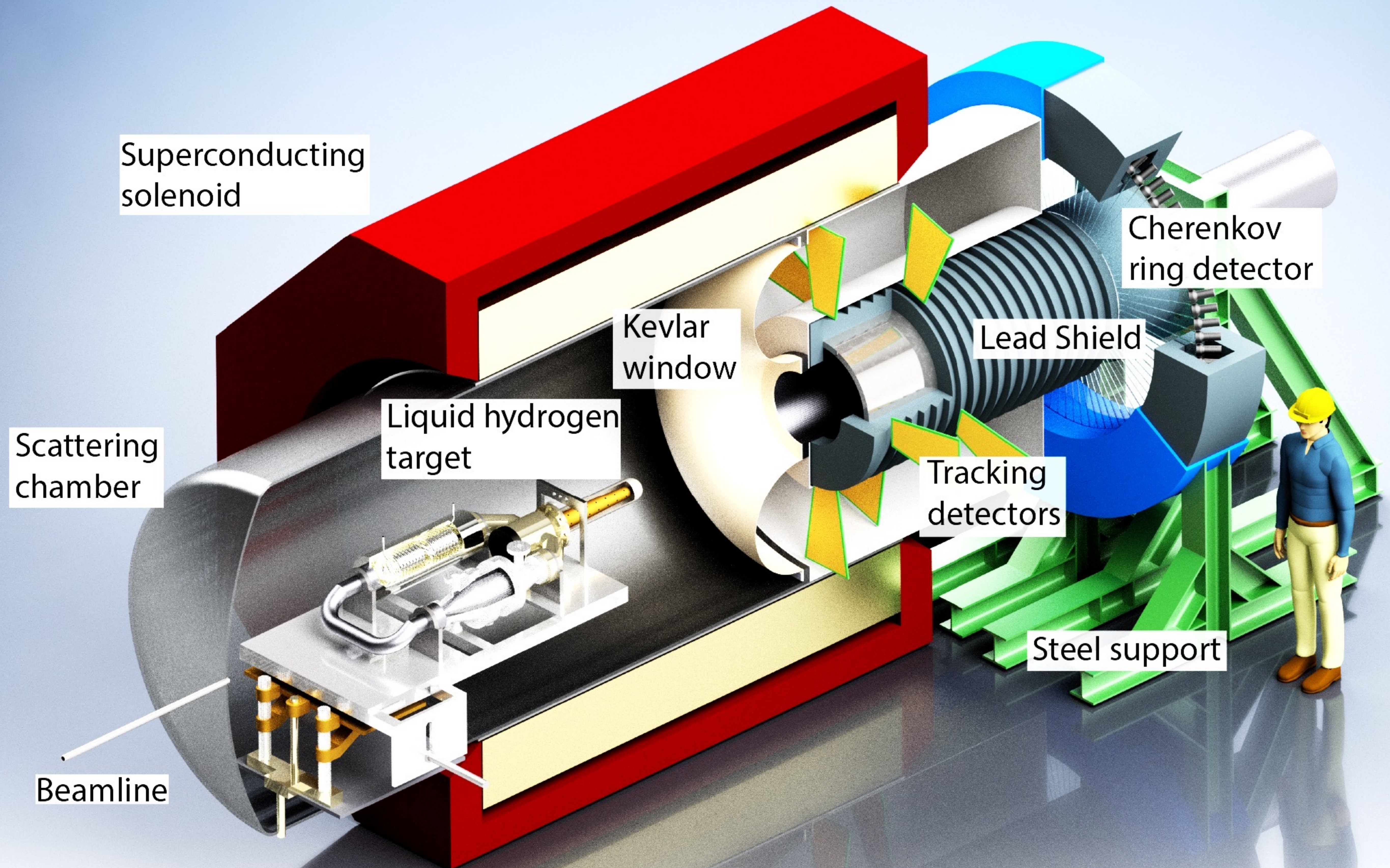

- First time use of a solenoid in PVES
- Magnet, Detector, and He-Refrigerator funded

Parity violating electron scattering

- 20 years of experience with previous parity violating electron scattering experiment (A4)
- 10000 h of beam and detector data
- 36 beam stabilisation systems
- Polarimetry, fast electronics, target

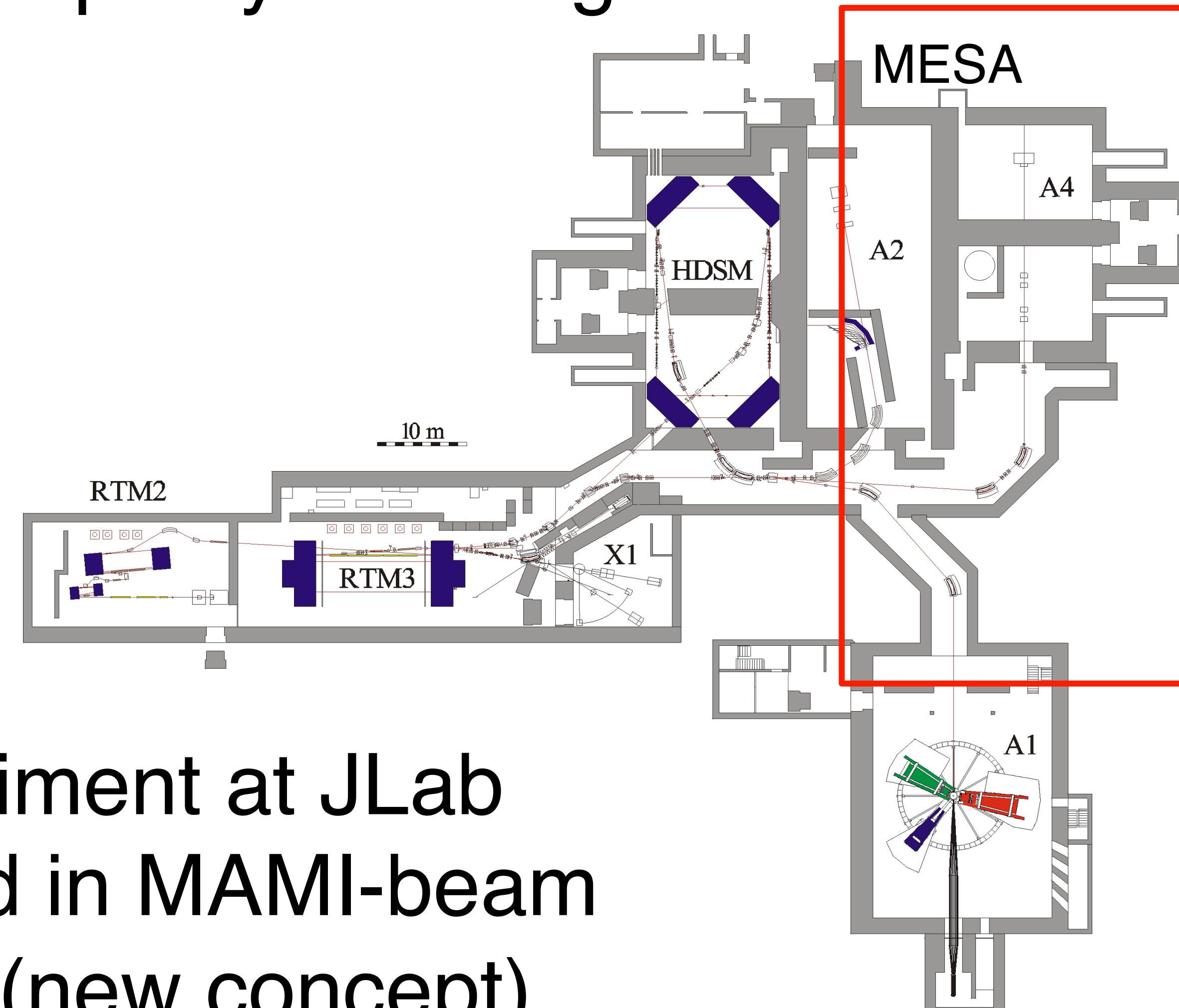

- MAMI accelerator in operation
- Large synergy with MOLLER experiment at JLab
- Prototypes of all components tested in MAMI-beam
- Integrating detectors and PMTs (new concept)
- Electronics and data acquisition (collaboration with Manitoba)
- Luminosity monitors
- Accelerator components, new concept position monitors
- Polarimetry (Hydro-Moller)

Recent publication from A4: B. Gou et al. *Phys.Rev.Lett.* 124 (2020) 12, 122003

Quartz glas detector concept

- Cherenkov detector ring consisting of **72 fused silica bars**
- Covering **full azimuth 25° - 45° polar angle**
- **Integrating detector**

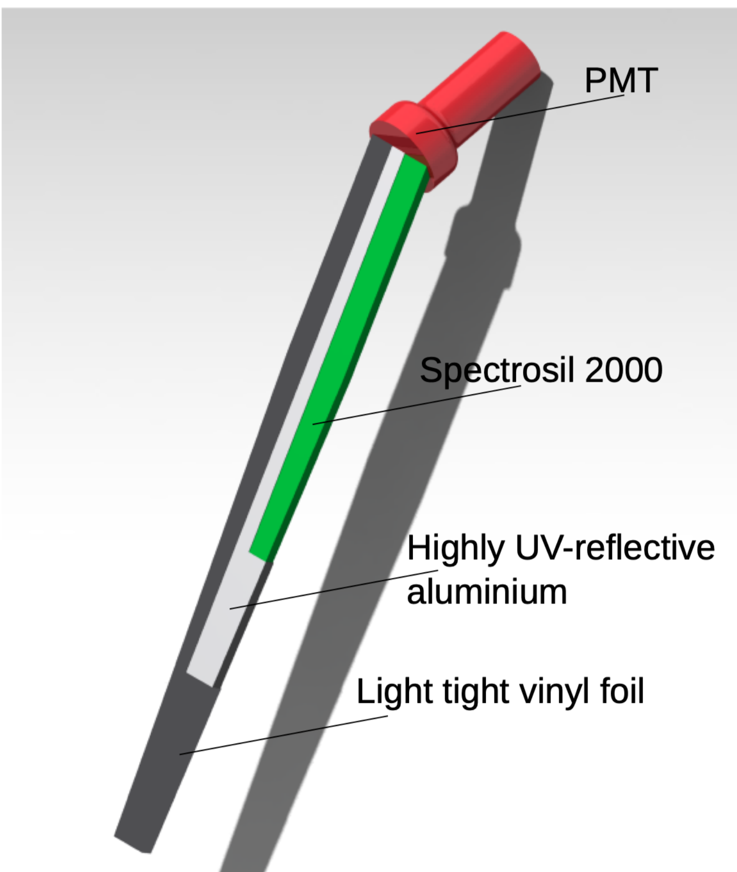

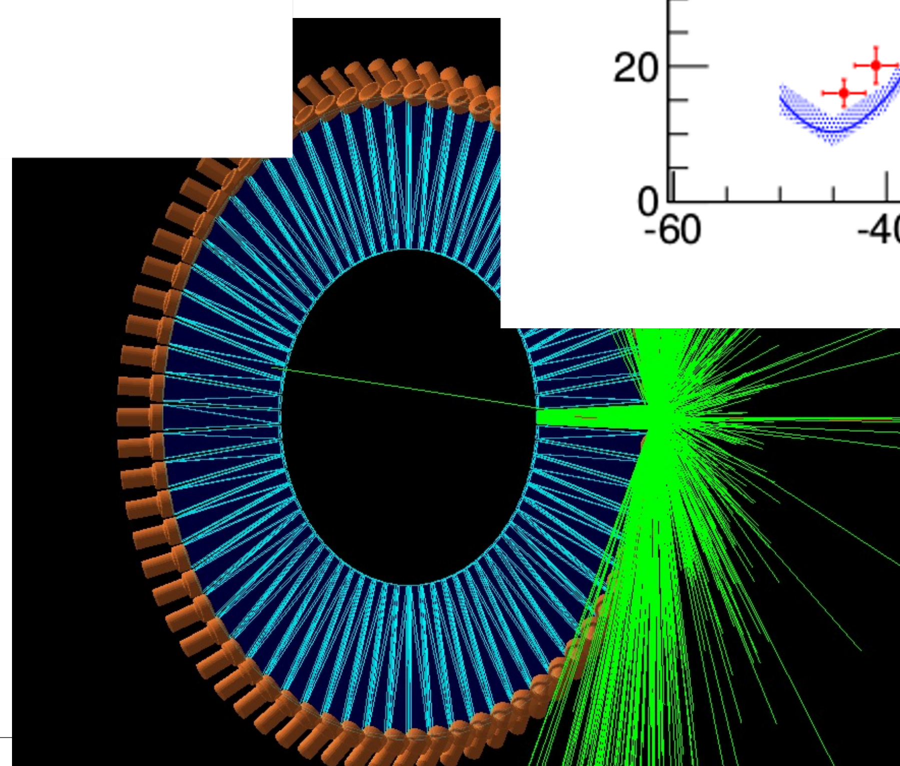

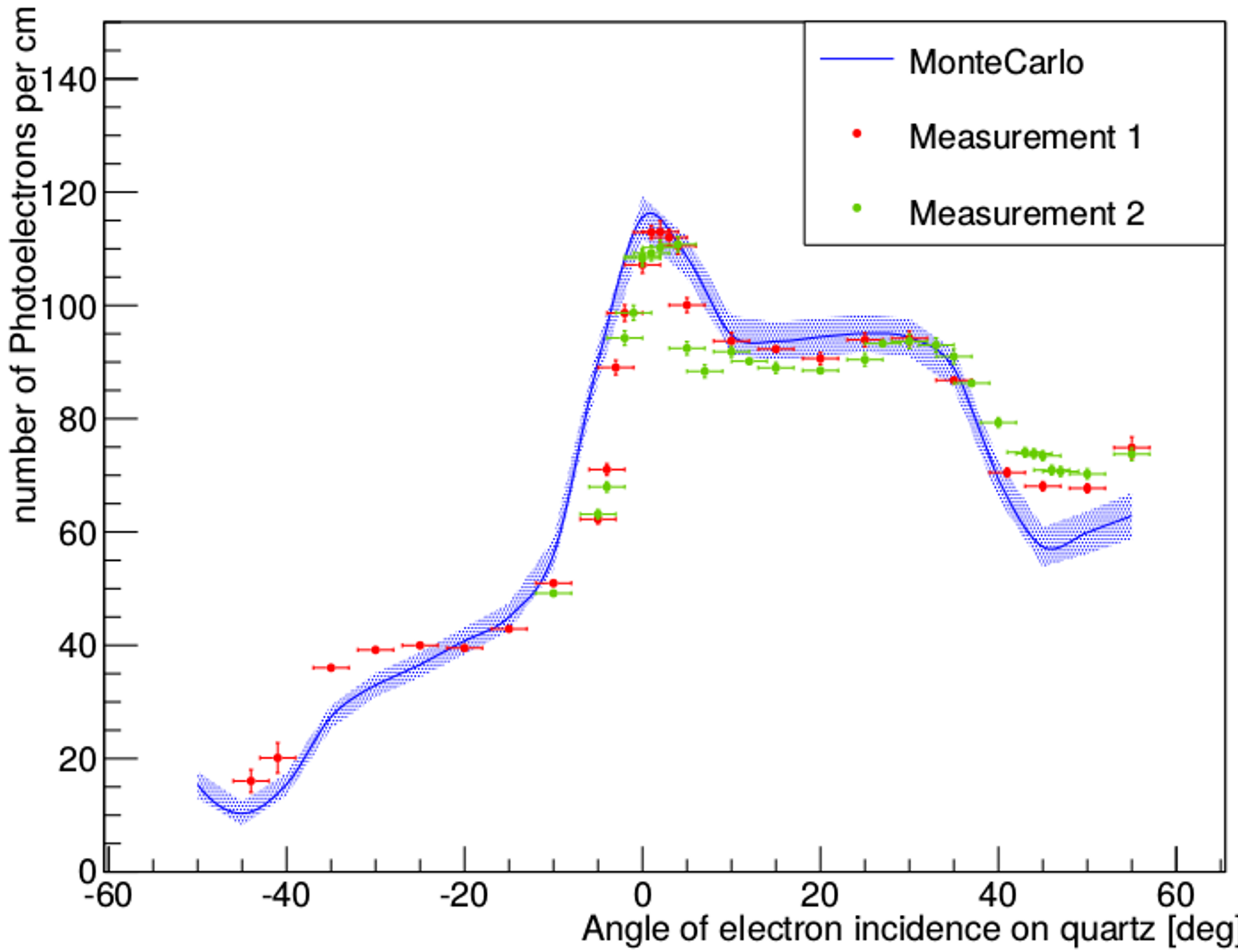

- Extended experimental study
- Quartz glas, PMTs, reflector
- Radiation hardness
- 500 h with MAMI beam

Spectrometer full simulation
Particles on quartz glass bar (proton)

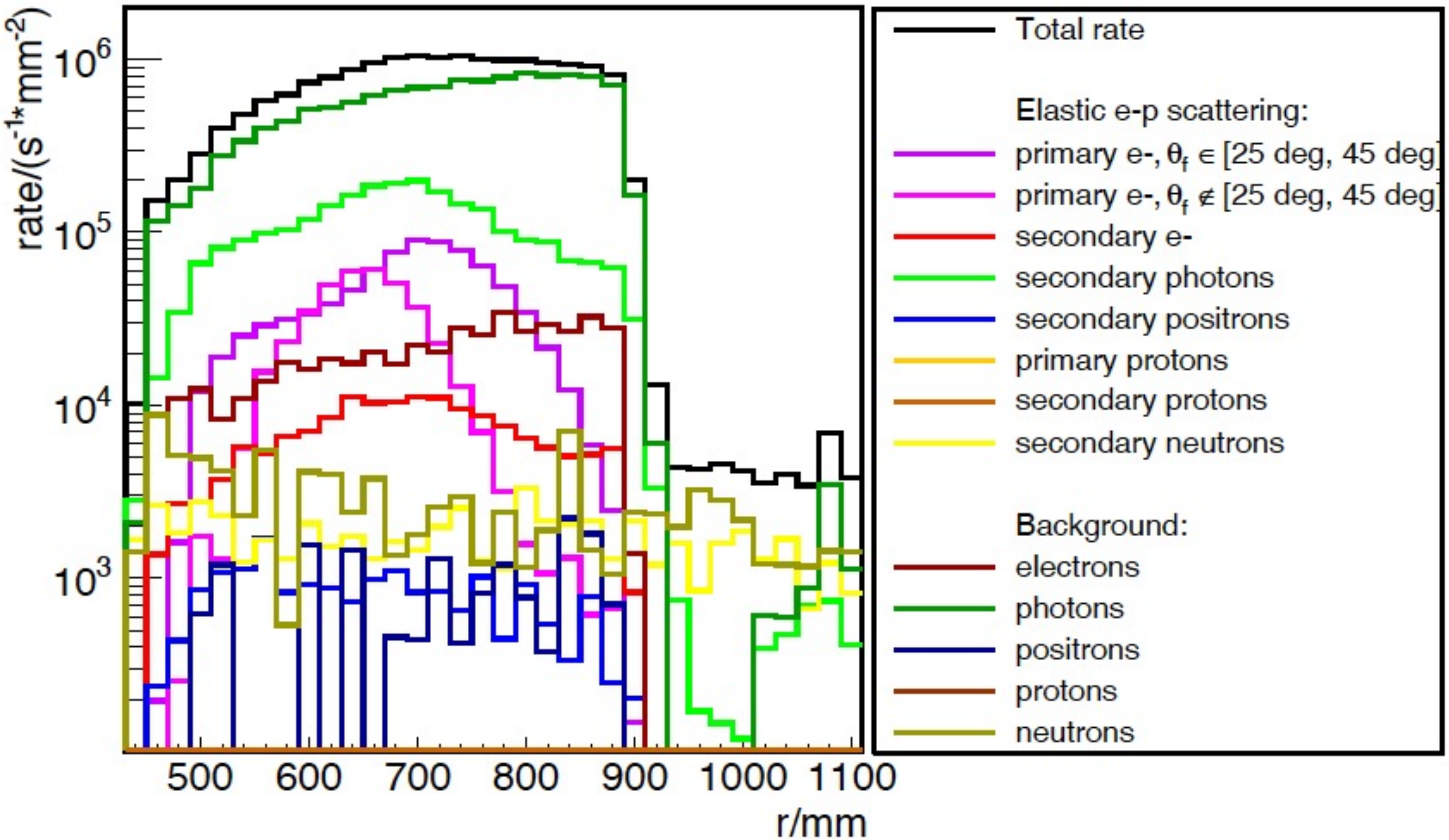

Spectrometer full simulation
Photo electrons on PMT (proton)

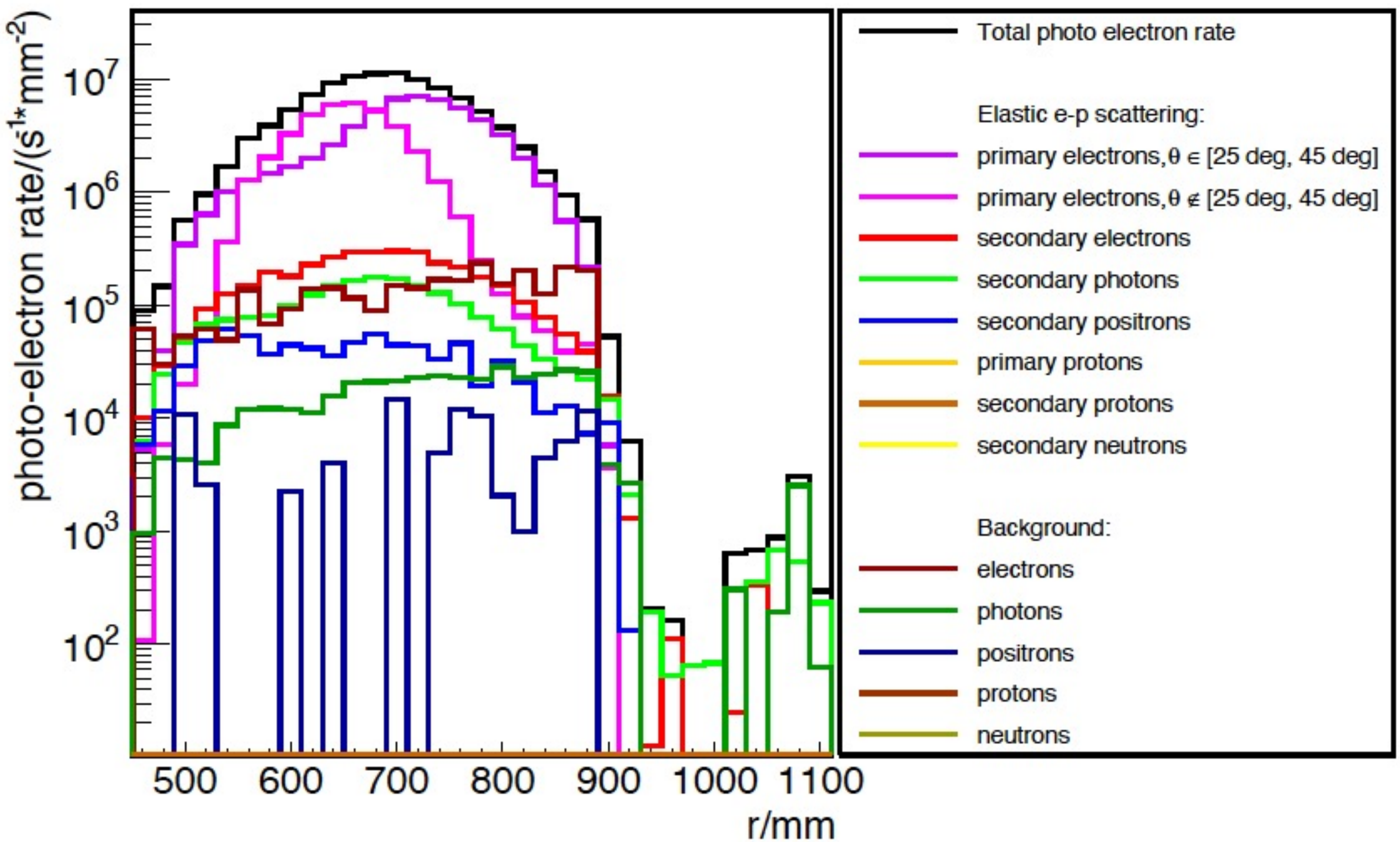

Spectrometer full simulation Photo electrons on PMT (proton)

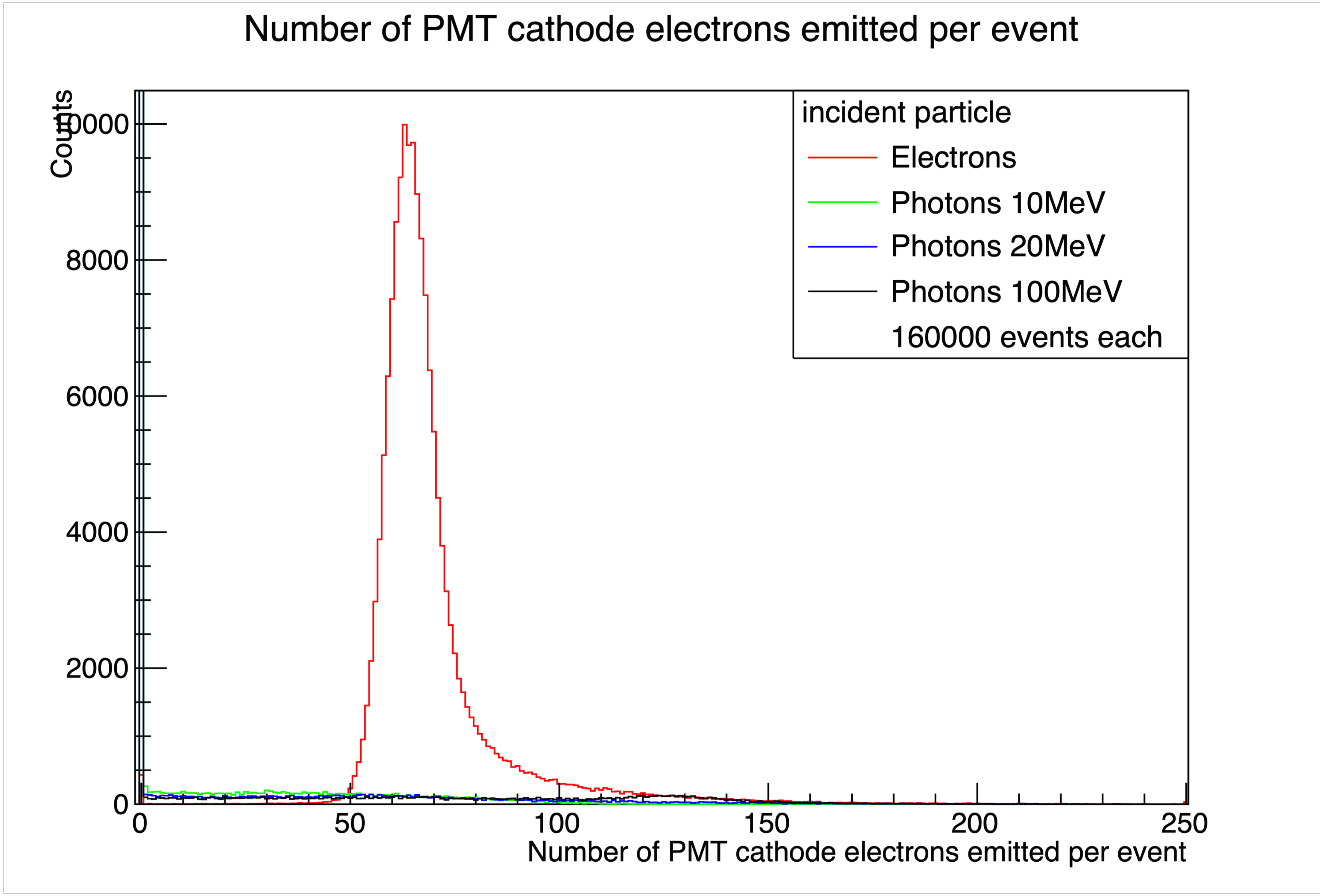

Q^2 tracking system

Momentum transfer Q^2 Tracking system

$$A_{LR}^{exp} = \frac{\sigma(e^{\rightarrow}) - \sigma(e^{\leftarrow})}{\sigma(e^{\rightarrow}) + \sigma(e^{\leftarrow})} = -P \frac{G_F Q^2}{4\sqrt{2}\pi\alpha}\left(Q_W(p) - F(Q^2)\right)$$

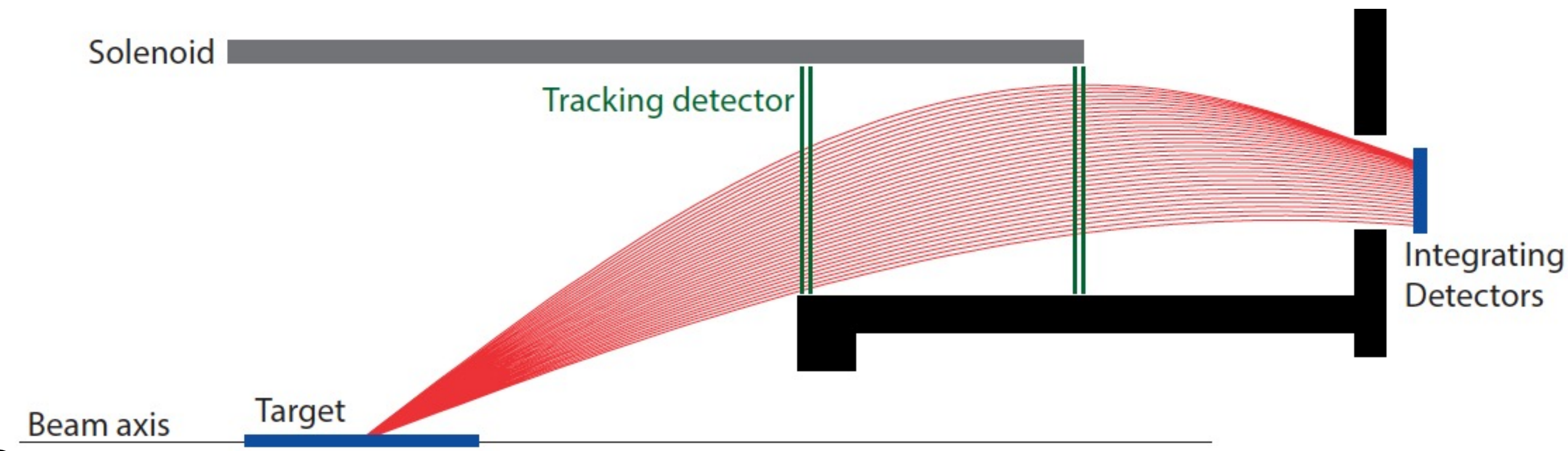

HV MAPS
50 μm thin silicon
1x2 cm fully
operational

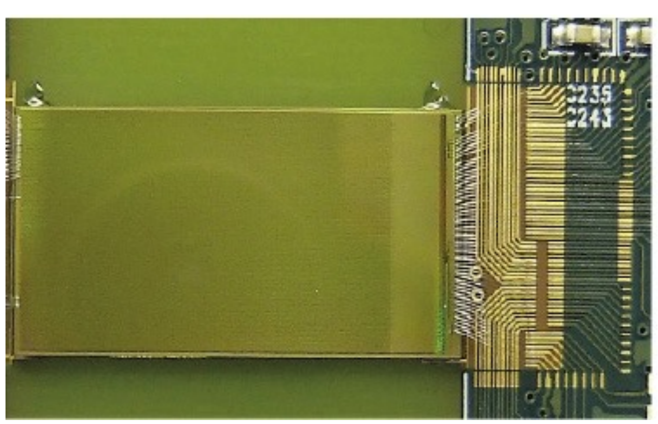

Full simulation
running

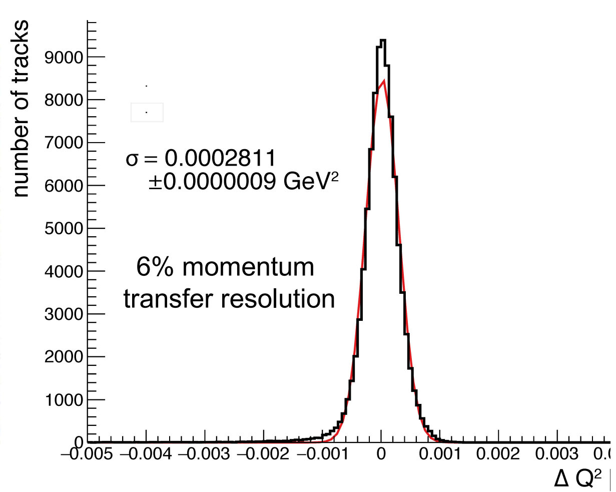

Thermo-mechanical
prototype

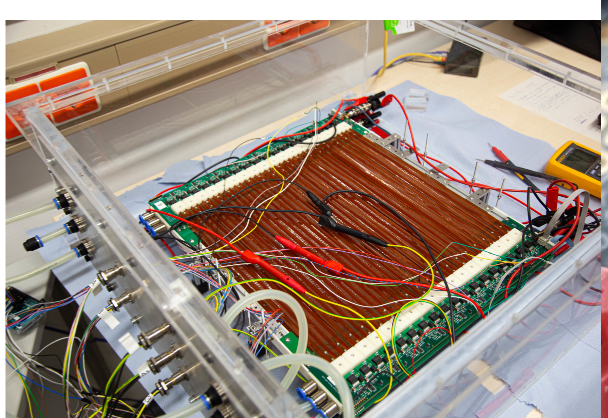

HV MAPS
50 μm thin silicon
2x2 cm available

P2 Tracking Detector

- Based on High-Voltage Monolithic Active Pixel Sensors (HV-MAPS)
- Full size sensors produced,
  work well (with Mu3e collaboration, beam tests at MAMI)

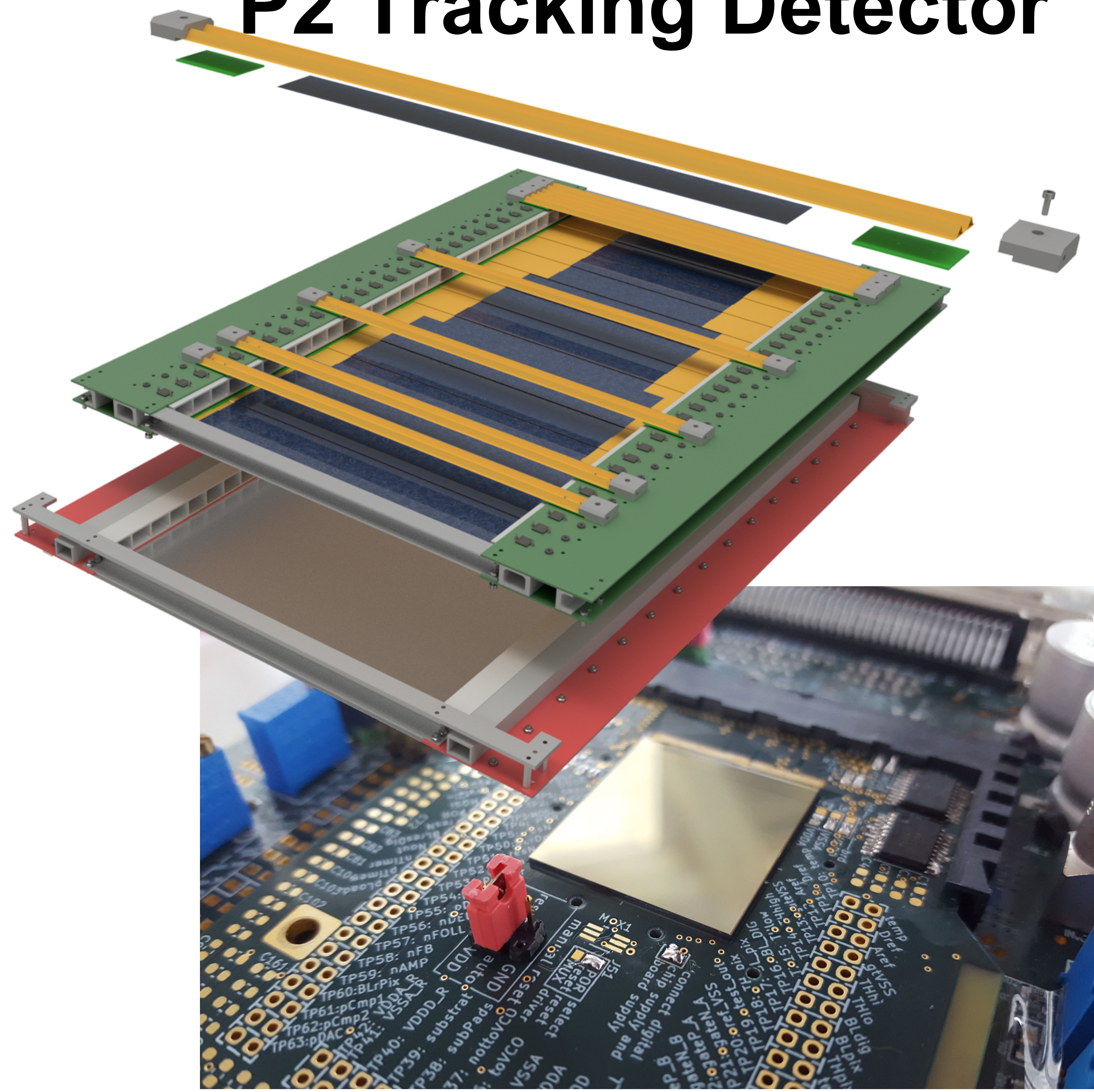

Das Bildelement mit der Beziehungs-ID rId51 wurde in der Datei nicht gefunden.

P2 Tracker Construction

- Remote powering solution under test (*Bachelor thesis Johannes Hoffmann*)
- Assembly and gluing robot for modules under construction in the PRISMA+ detector lab (*Bachelor theses Patrick Riederer, Jana Weyrich, David Anthofer*)
- Cooling optimized and experimentally verified

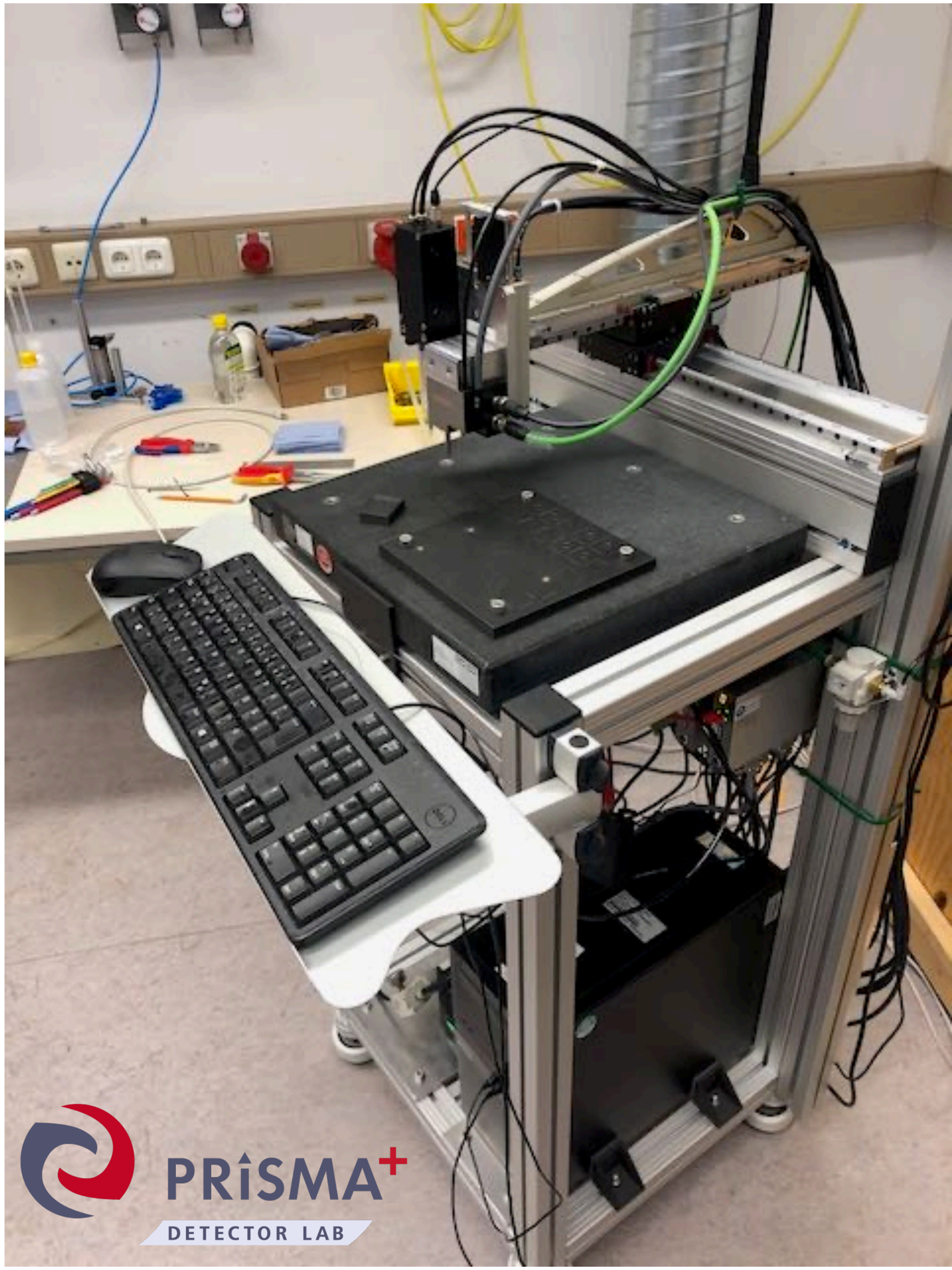

Das Bildelement mit der Beziehungs-ID rId51 wurde in der Datei nicht gefunden.

Set up at the MAMI accelerator

Test of analogue integrating readout

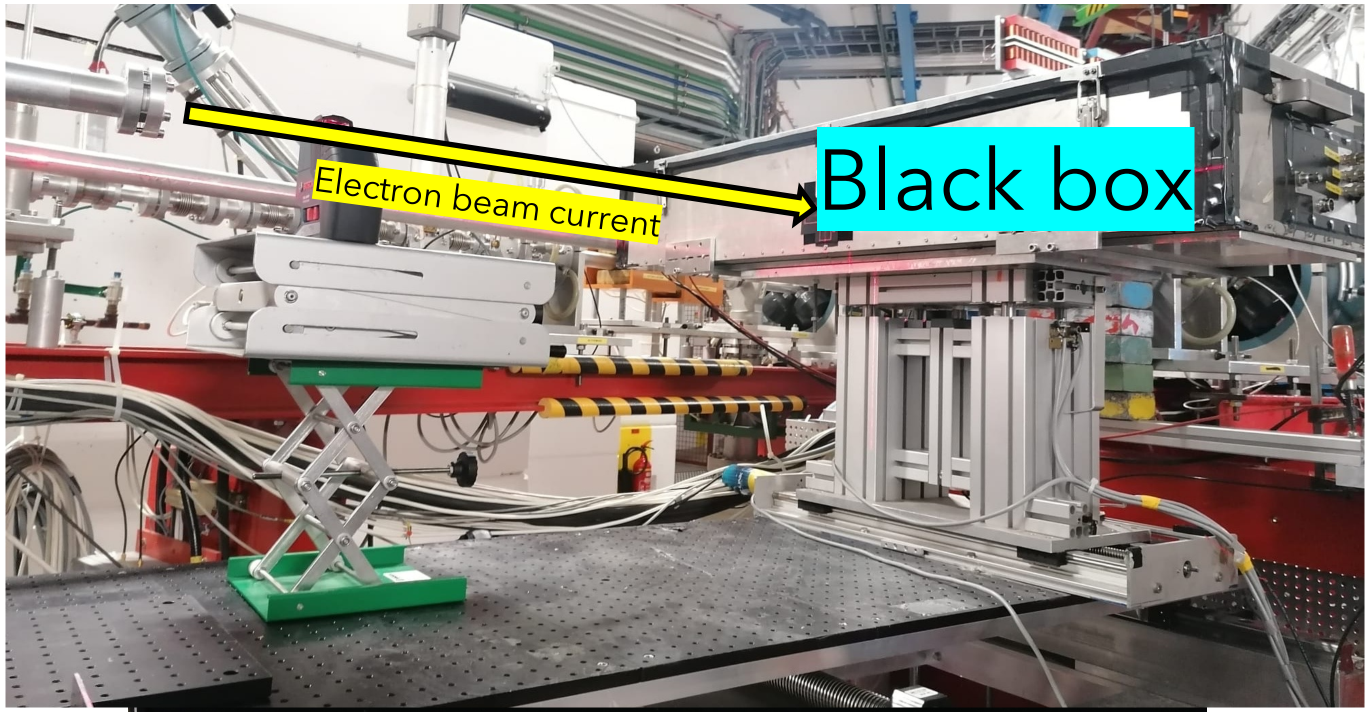

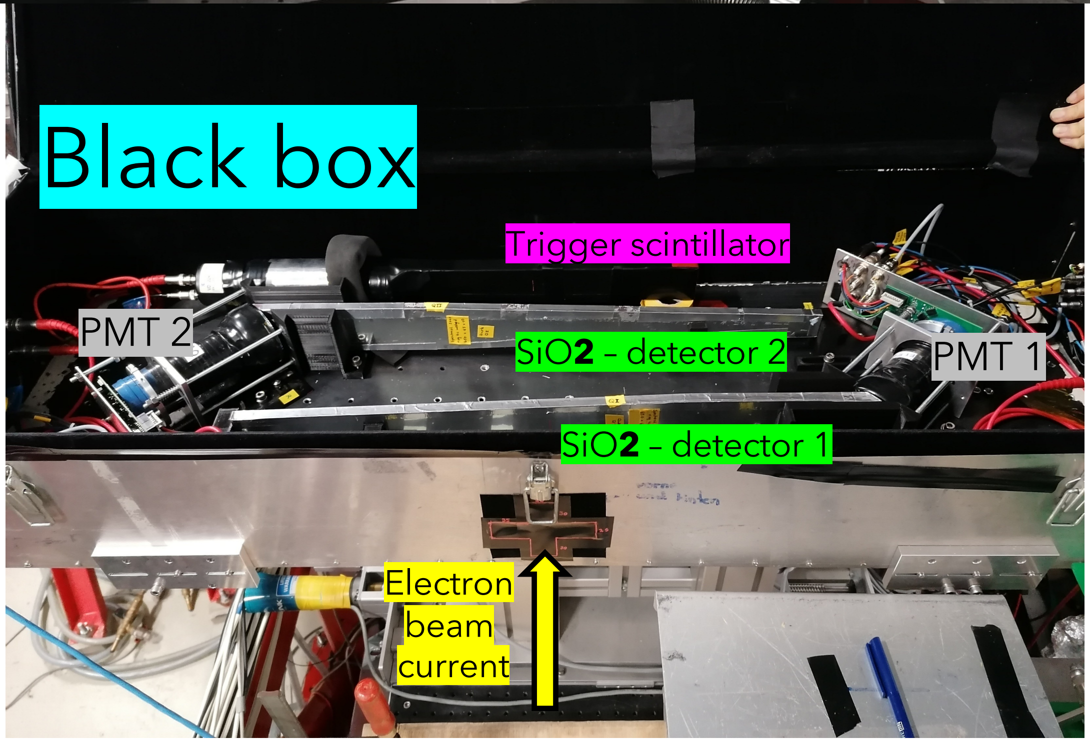

Das Bildelement mit der Beziehungs-ID rId51 wurde in der Datei nicht gefunden.

Counting single electrons

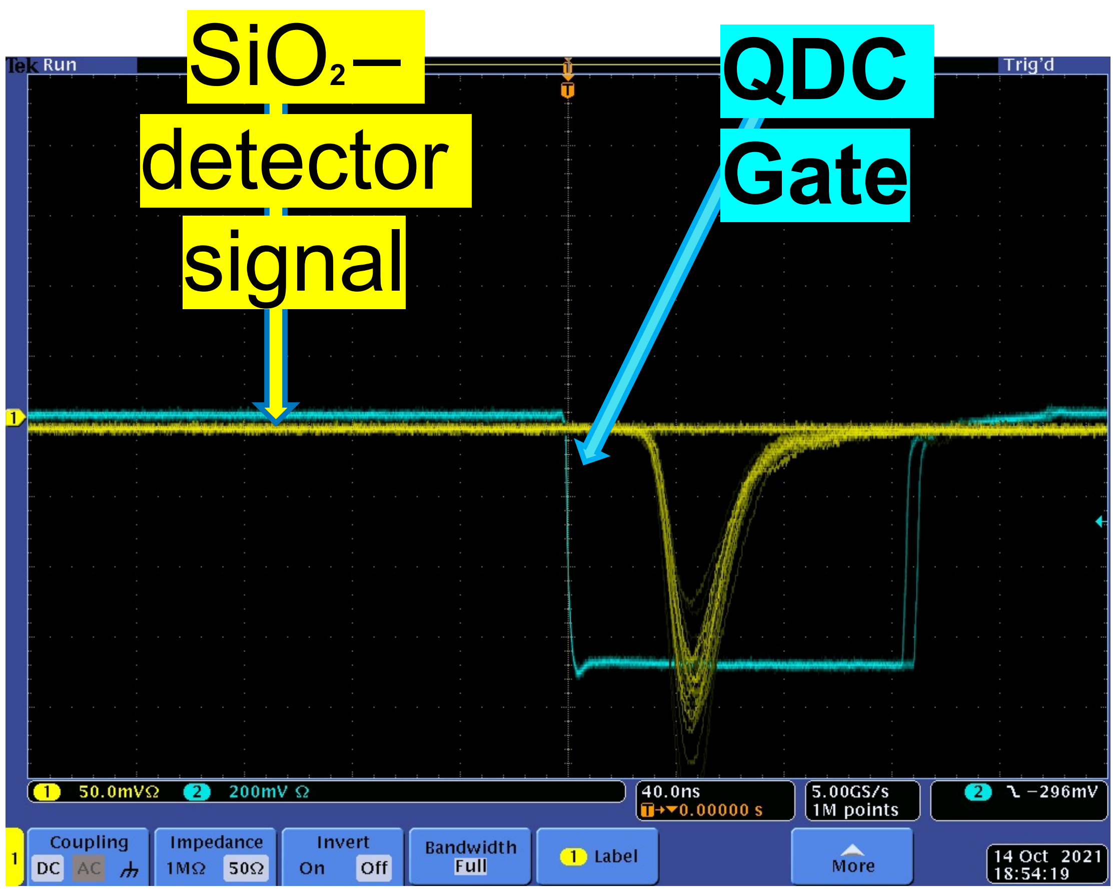

Electron beam rate = 2,0 kHz
SiO2 detector voltage = -825 V (nom. voltage)
Oszi Trigger: Trigger scintillator

QDC spectrum of SiO_2 detector

QDC: Charge-to-Digital-Converter

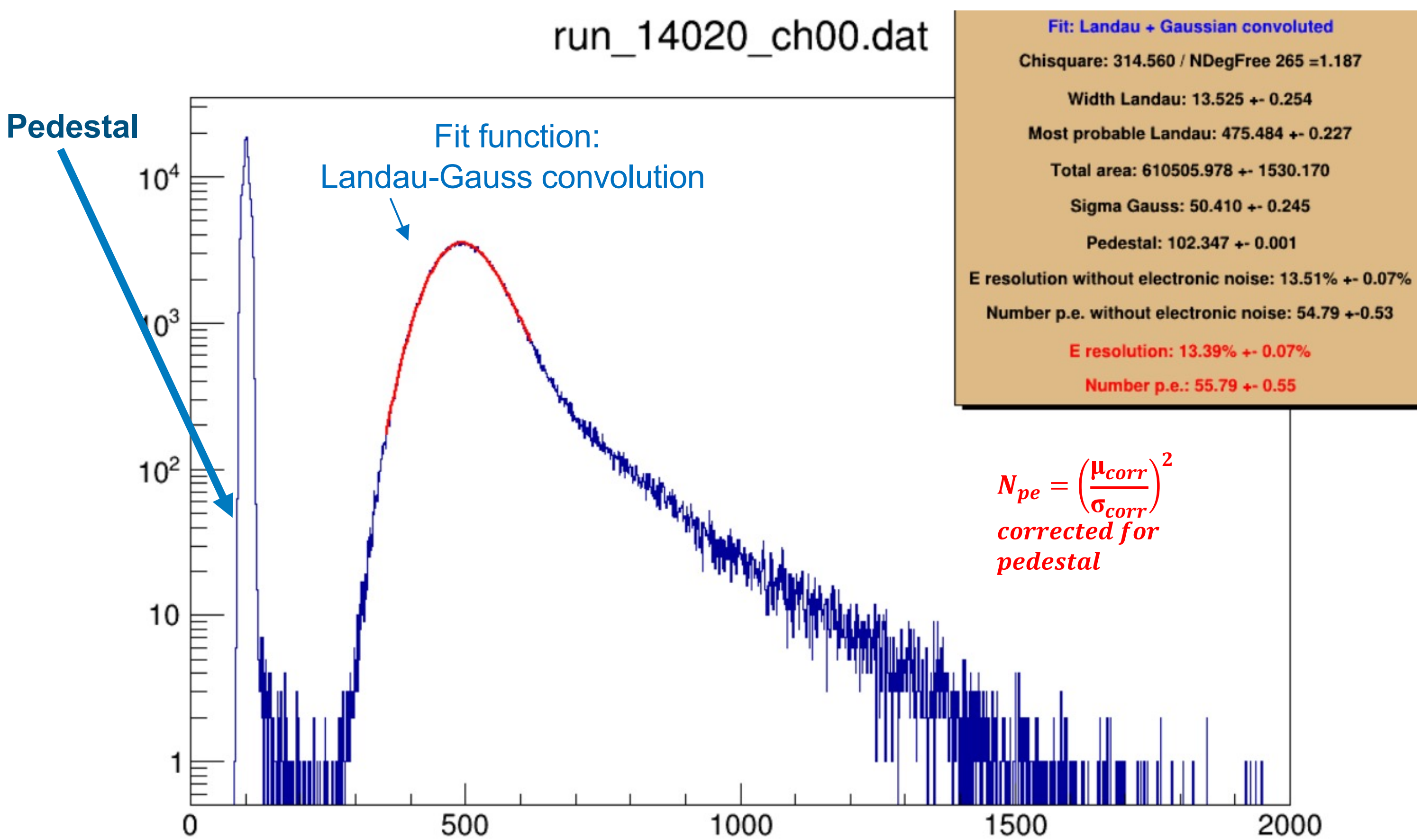

Electron beam rate = 2,0 kHz
SiO2 detector voltage = -827 V (nom. voltage)
DAQ Trigger: Trigger scintillator

Das Bildelement mit der Beziehungs-ID rId51 wurde in der Datei nicht gefunden.

Integrating single electrons (analogue measurement)

Measurement with electron beam current at MAMI

Electron beam current = 274 pA ≈ 1,69 GHz

PMT operating voltage = 500 V

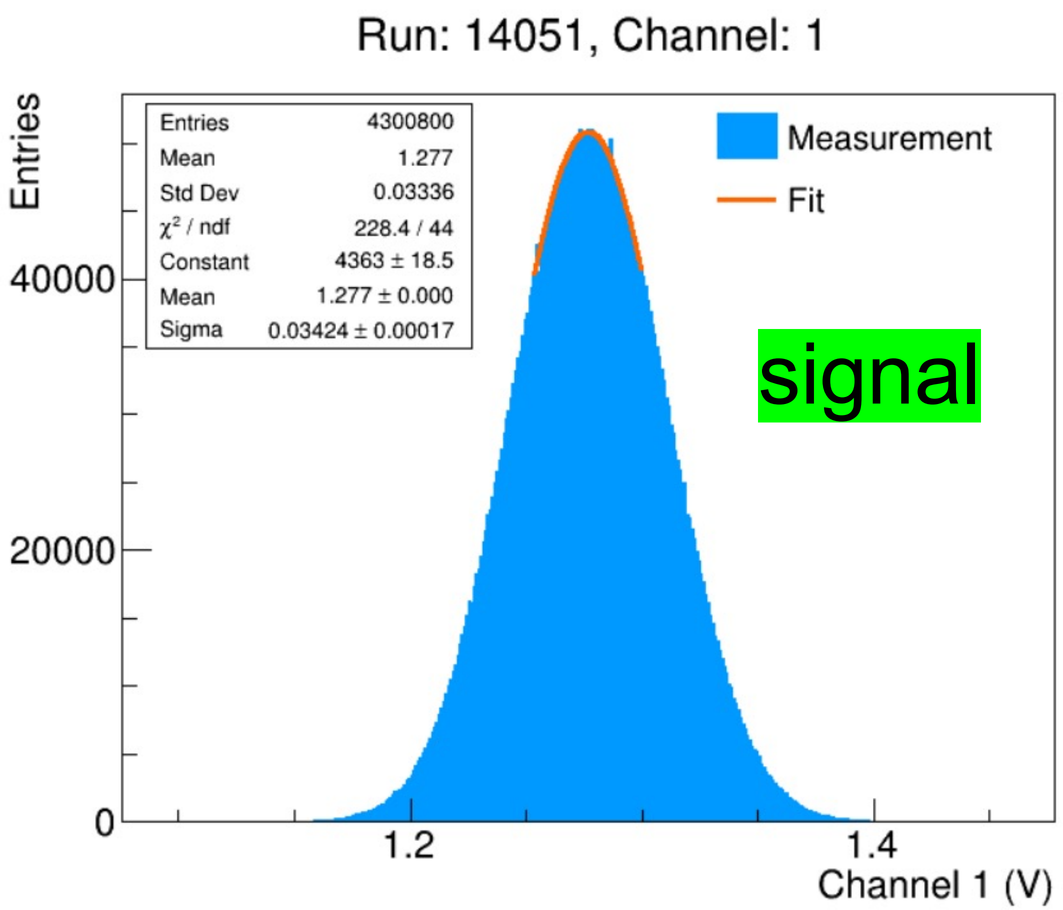

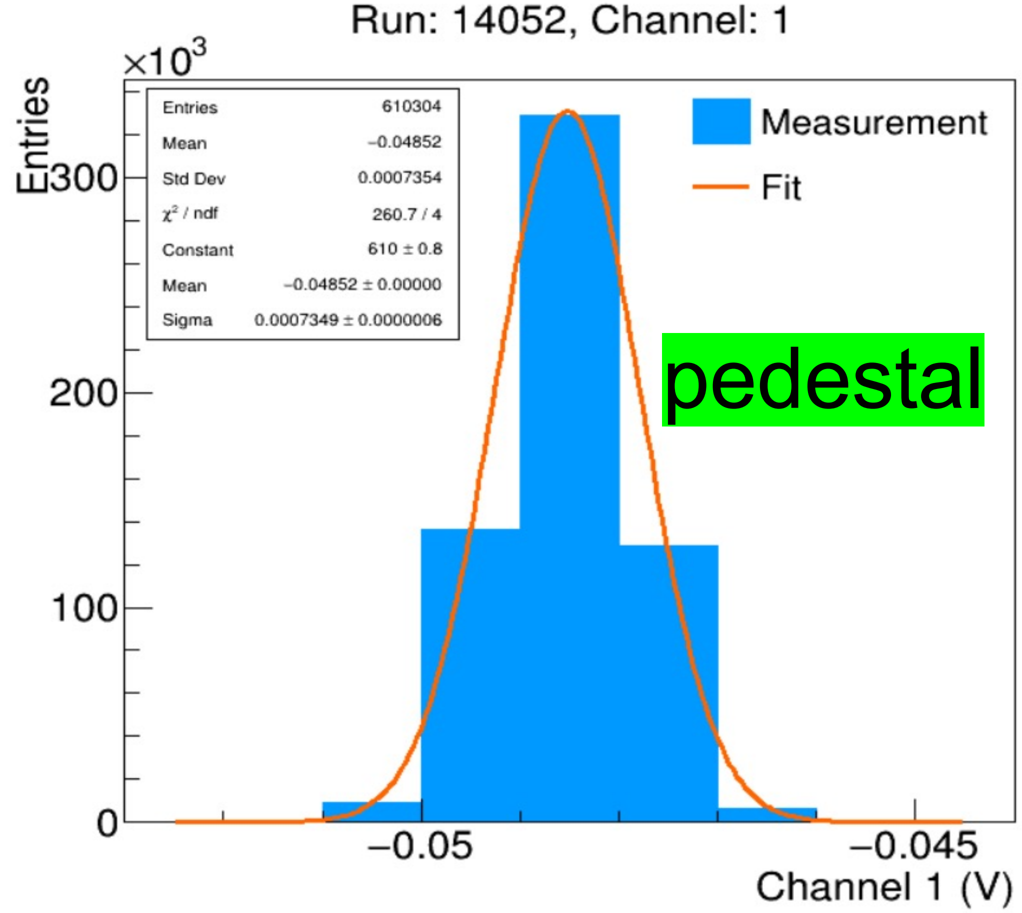

Das Bildelement mit der Beziehungs-ID rId51 wurde in der Datei nicht gefunden.

Integration Mode: Linearity Test

Measurement with electron beam current

Electron beam current at SiO_2 detector

PMT operating voltage = 500 V PMT

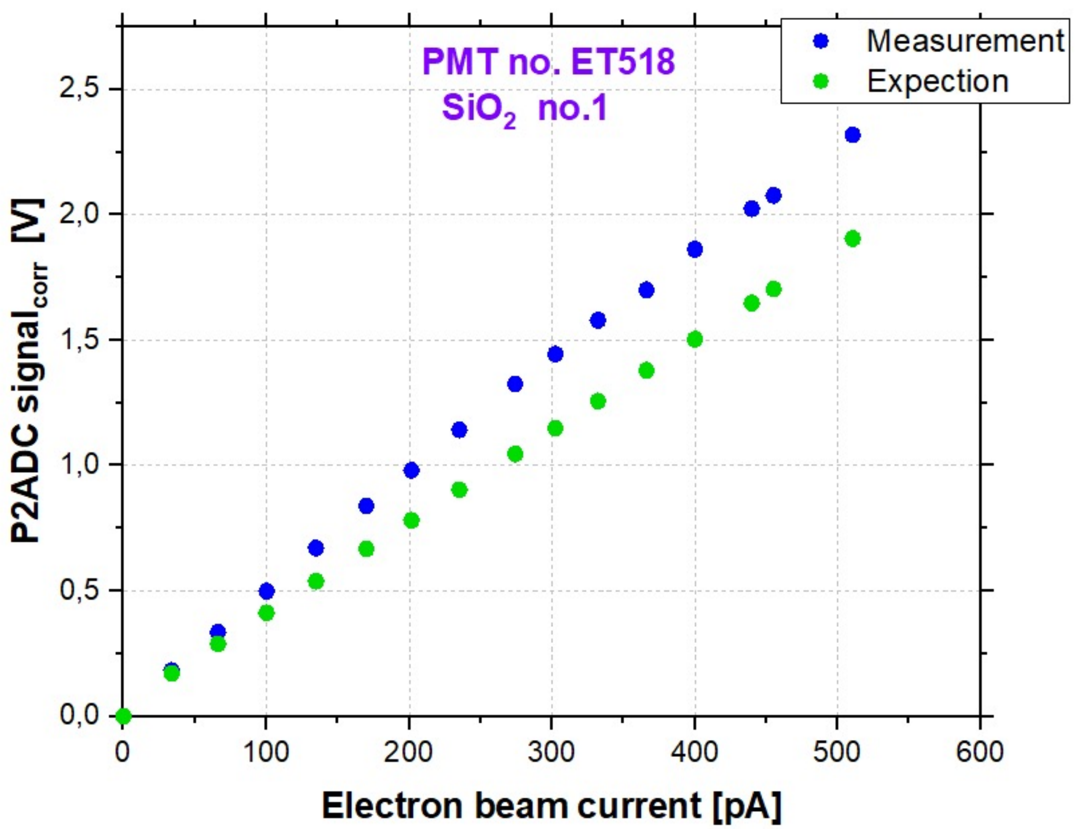

Das Bildelement mit der Beziehungs-ID rId51 wurde in der Datei nicht gefunden.

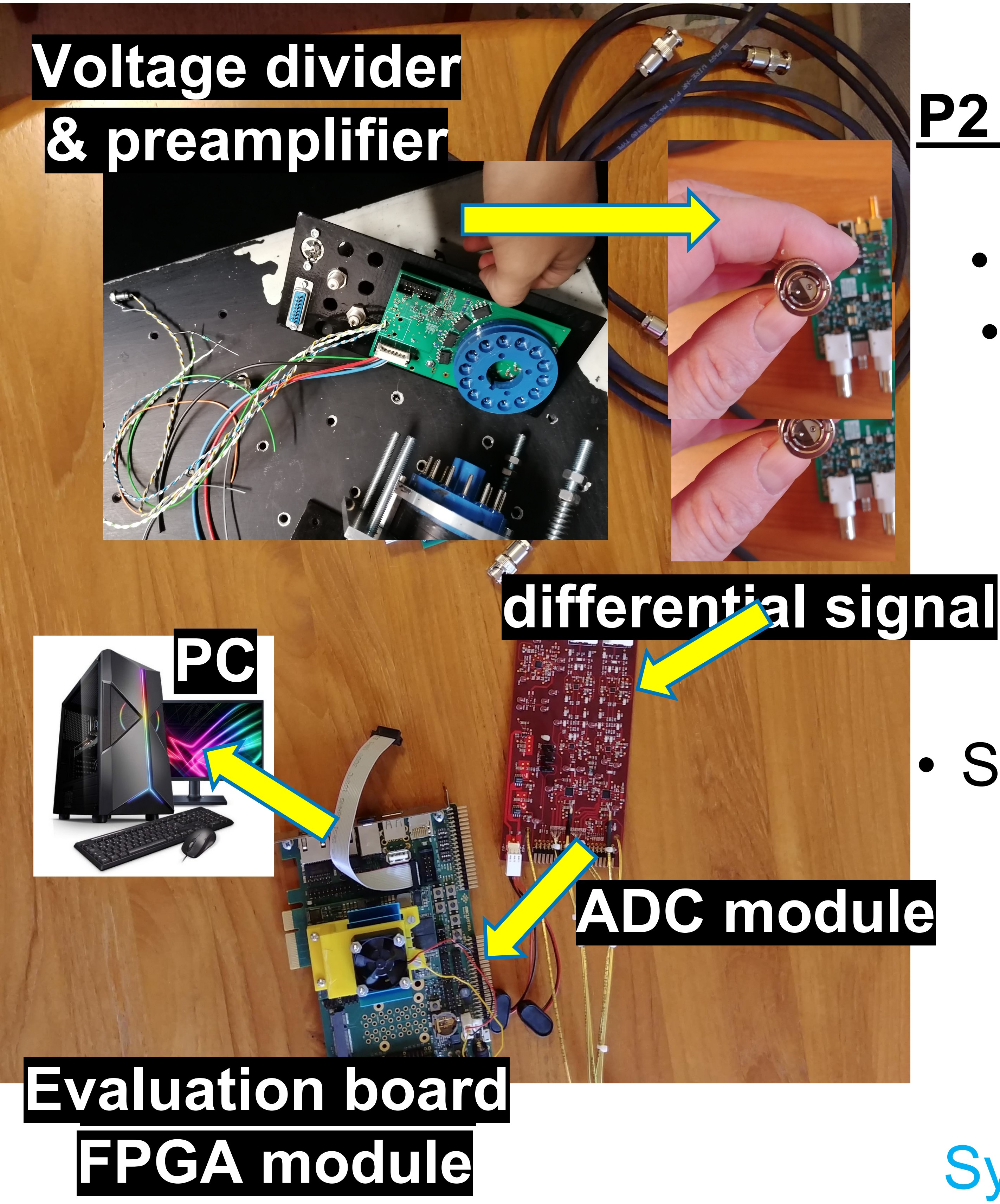

Prototypes of full differential read-out electronics

P2 voltage divider and preamplifier

- Single Event Mode: 10 dynodes
- Integration Mode: 5 dynodes
- Feedback resistor: 33 kOhm
- Differential output at preamp

P2ADC basic parameters

- Synergy with University of Manitoba
- ADC prototype for P2
- 18-bit
- Dynamic range of +/- 4.096 V

Synergy with University of Manitoba

Das Bildelement mit der Beziehungs-ID rId51 wurde in der Datei nicht gefunden.

Integration Mode
Measurement with electron beam current at MAMI

Electron beam current = 274 pA ≈ 1,69 GHz
PMT operating voltage = 500 V

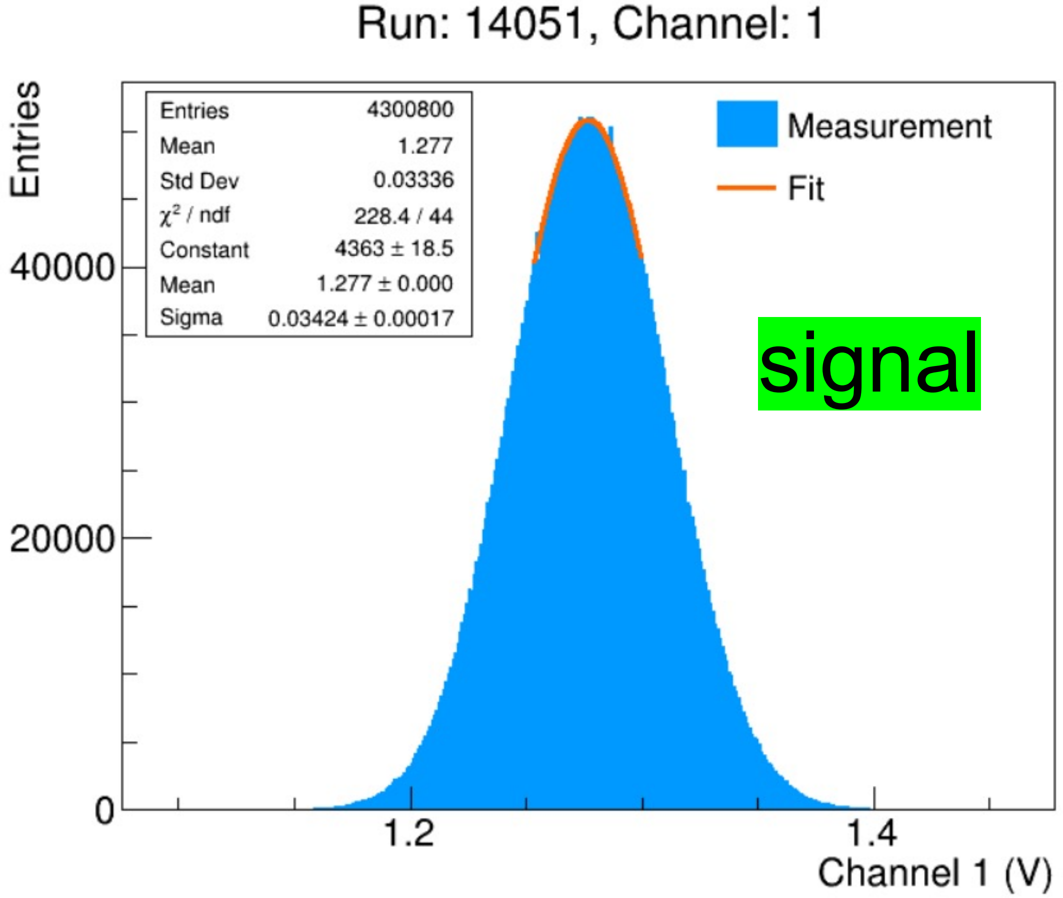

Signal as a function of time:
Samples taking in the first 300 us

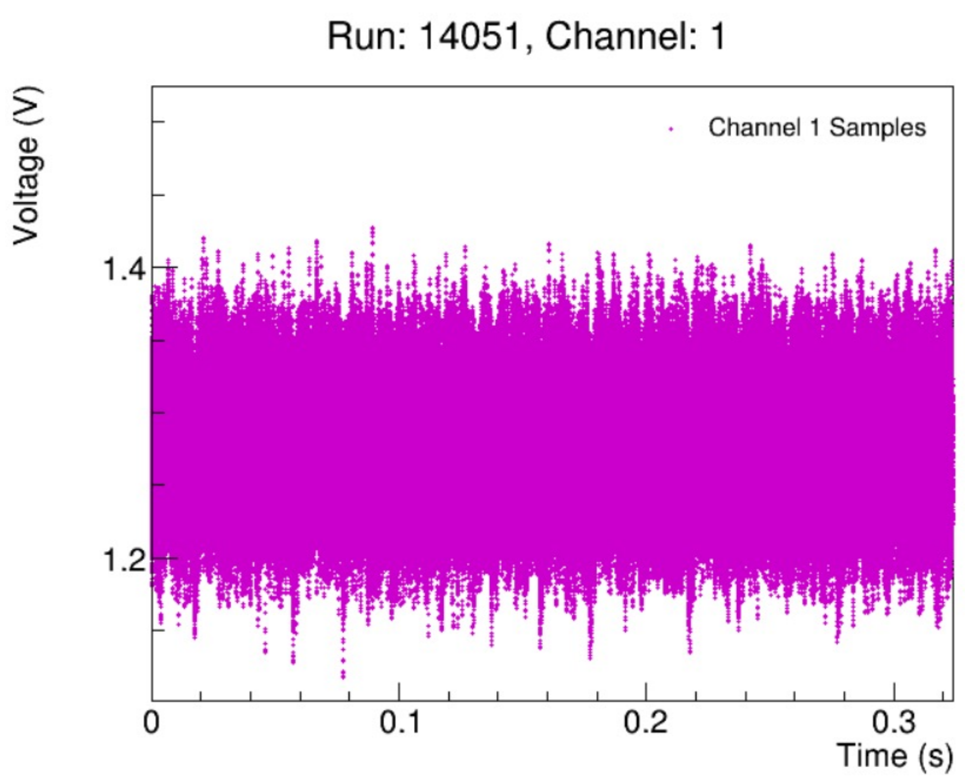

Test of analogue integrating detector and readout

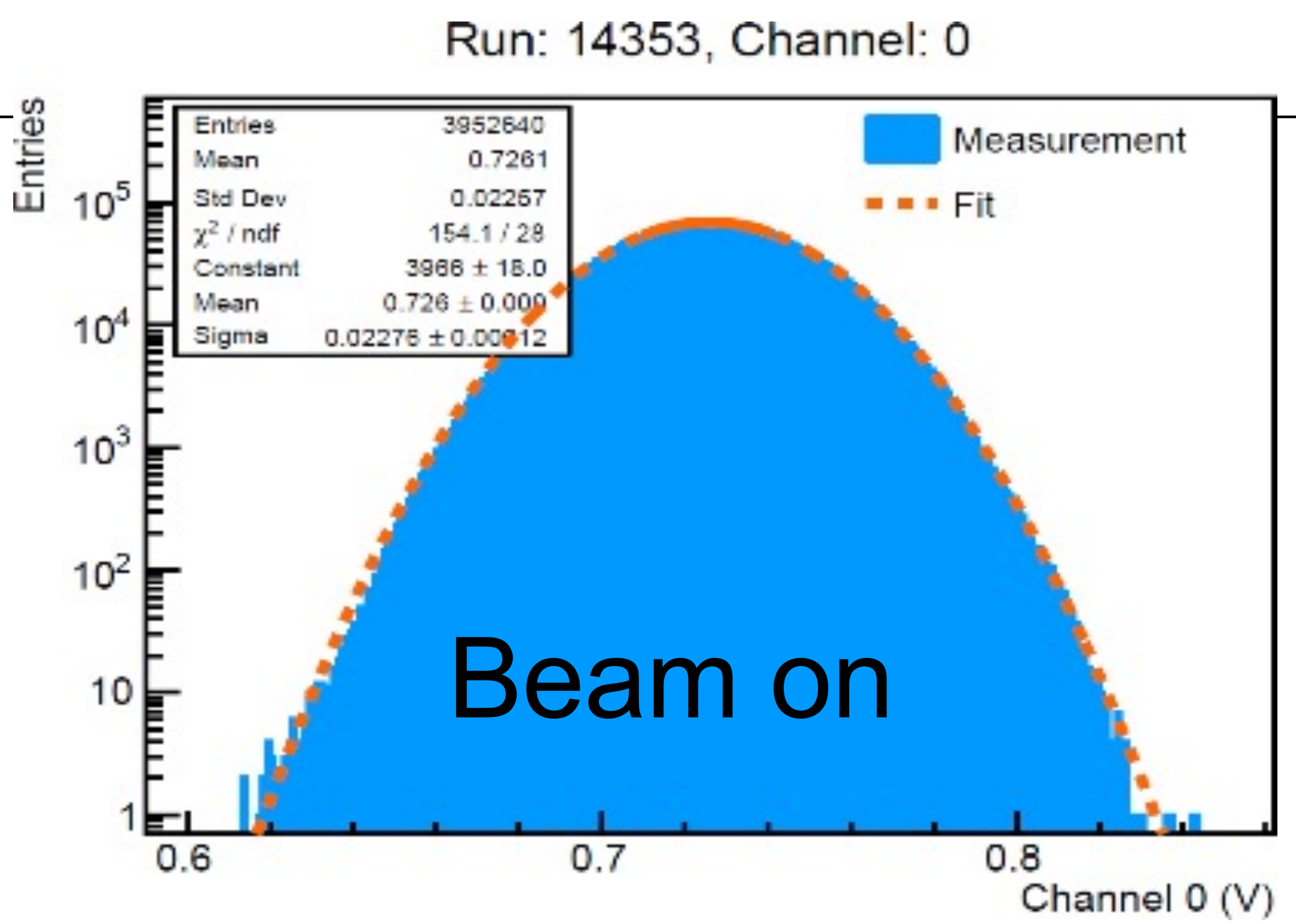

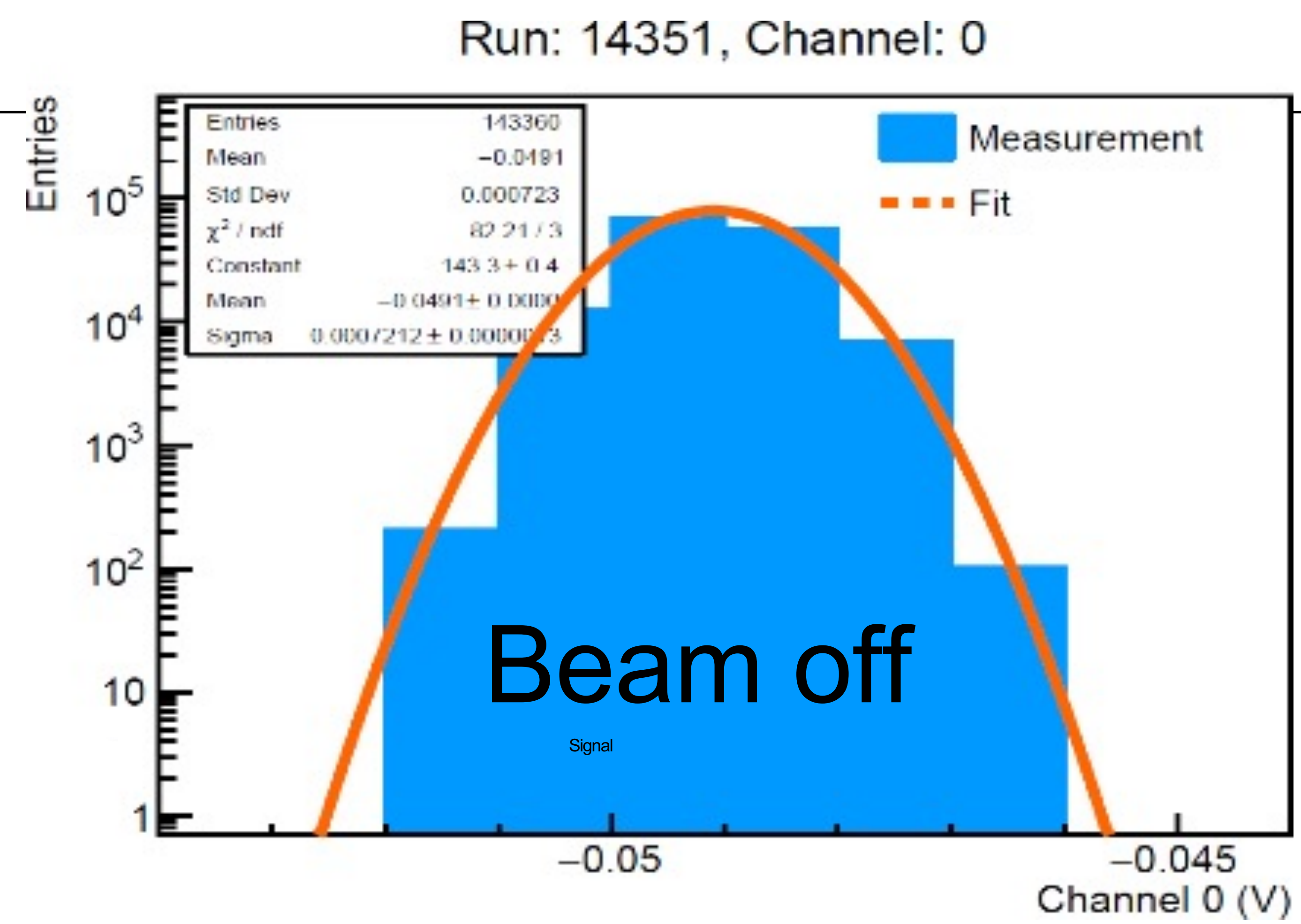

- Analogue signal from electrons in quartz Cherenkov, 274pA=1.7 GHz electrons on detector
- Electronics from U Manitoba
- Response of detector and width as expected
- System is ready to be used in the experiment

Measurements

Parity violating electron scattering Measurements: Use of beam time

- Challenging measurements
- Unknown: New accelerator MESA (performance of SC RF)
- Parity-grade beam properties needed

- Unknown: Commissioning of accelerator and the two main experiments in parallel (MESA, MAGIX, P2)

Strategy:
- Start with large asymmetries, easy targets
- First Phase: Pilot measurements with reduced statistics but meeting or improving previous experiments
- Second Phase: Aim for ultimate precision
- A total of about 16,000 h: 6 years to complete measurements 2025 - 2030

	A $[10^{-9}]$	ΔA $[10^{-9}]$	Data taking time	Q^2 $[(GeV/c)^2]$	Angle interval	Comment	When
H_2-I	40	0.8	1000	0.005	25° – 45°	Pilot measurement, reach Qweak accuracy	
C-I	400	15	1000	0.005	30° – 40°	Pilot measurement with larger Asymmetry, 4% accuracy	
Pb-I	660	7	800	0.007	30° – 40°	Pilot run to reach same statistics as Prex-II, in EOS	
H_2-R	4500	70	1000	0.06	140° – 150°	Backward angle measurement to improve G_A und G_M^s , needed to reach the final goal for $\sin^2\theta_W$	
D_2-R	4500	70	1000	0.06	140° – 150°	Backward angle measurement to improve G_A und G_M^s , needed to reach the final goal for $\sin^2\theta_W$	
H_2-II	40	0.3	9000	0.005	25° – 45°	Complete Statistics (including first meaurement) to reach final goal for $\sin^2\theta_W$	
C-II	400	8	1500	0.005	30° – 40°	Complete Statistics (including first meaurement) to reach final goal for $\sin^2\theta_W$	
Pb-II	660	7	800	0.007	30° – 40°	Complete full statistics run would be highly desirable,	208ff

Risk in schedule due to unknown accelerator performance

Carbon simulations

- Raytracing simulation
  - Geant 4
  - Fast simulation
  - No real target, only virtual
  - Using mean energy loss
  - No multiple scattering
  - No secondary particles
  - Only absorber
  - Tracing the primary electron

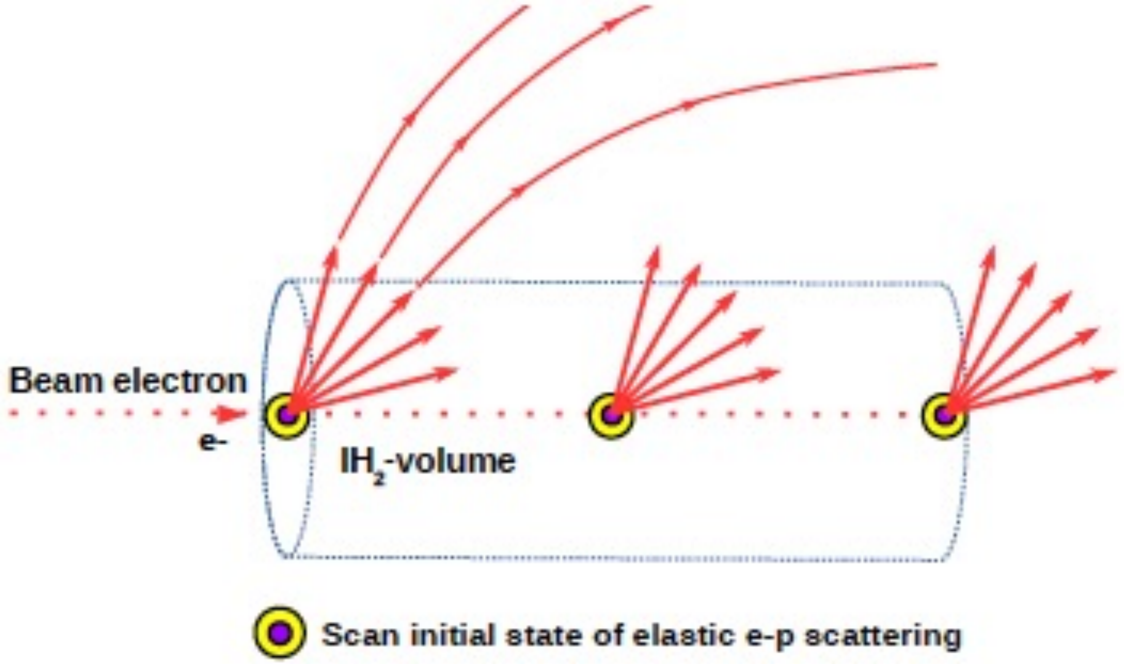

- Full simulation (P2Sim)
  - Geant 4
  - Slow simulation
  - Real target
  - Real energy loss
  - Multiple scattering
  - Secondary particles
  - Full setup
  - Track all particles

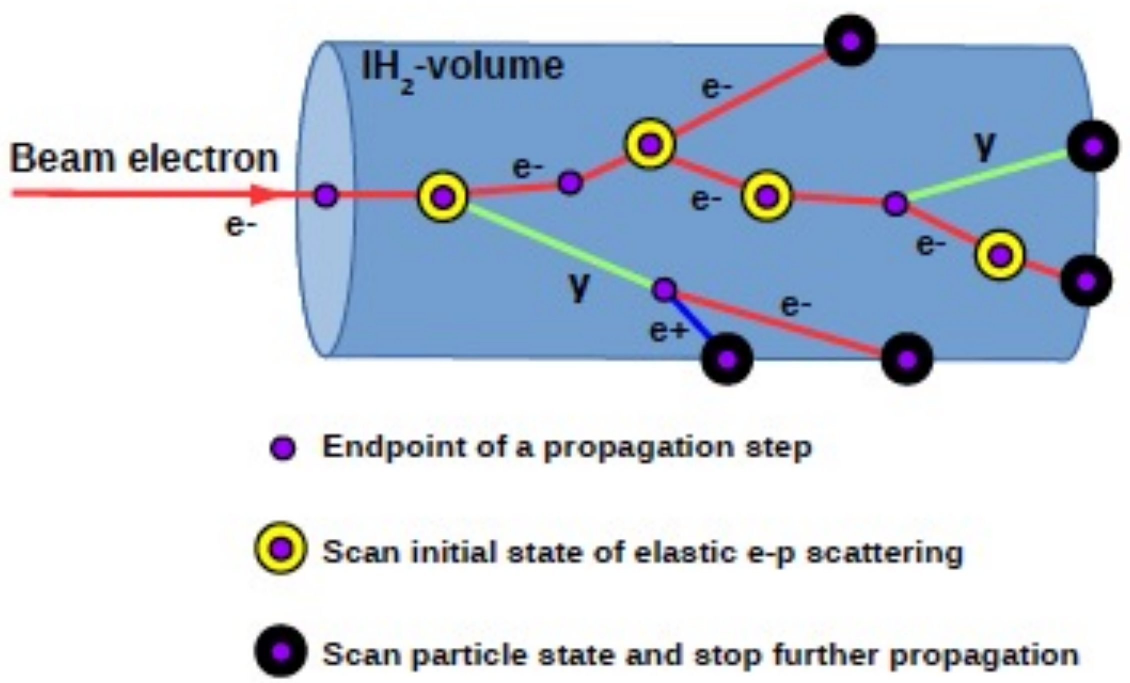

Carbon simulations

- Target centre at lH2 position
- Elastic scattered electrons
- Inelastic scattered electrons
- Using a 5-finger target
  - Thickness: 4.4 mm
  - Separation: 36 mm
- Focusing point
- Separation between elastic and inelastic scattering

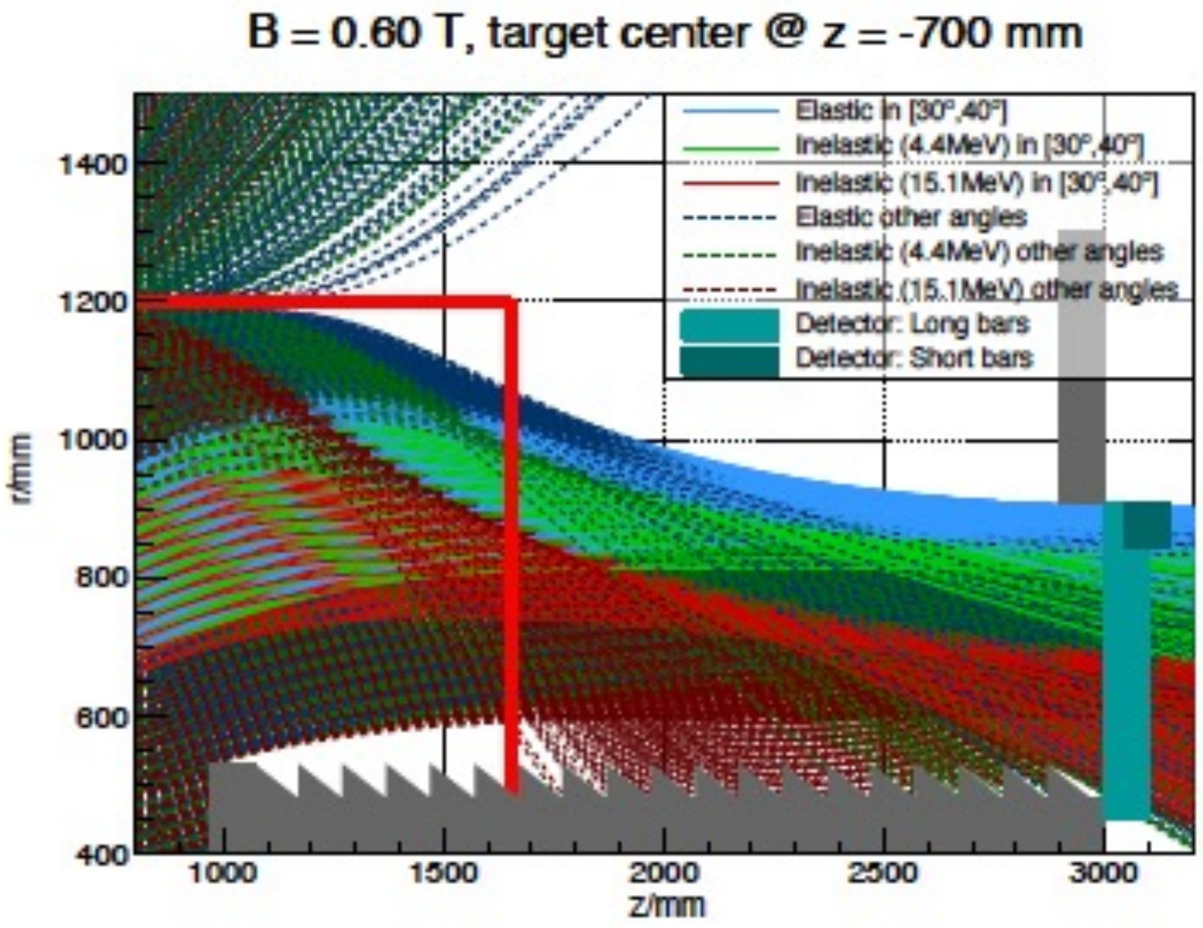

- Shorter quartz glas detector as compared to Hydrogen
- Cross section for inelastic scattering from excited states 10^{-4} suppressed

Carbon simulations

- Inelastic scattered electrons
  - Sum from 4.4, 7.6, 9.6 MeV states
  - Located at smaller *r*
- Rate dominated by photons
- Photoelectron rate dominated by primary electrons
- Separation between elastic/inelastic electrons possible

⇒ Use short bars

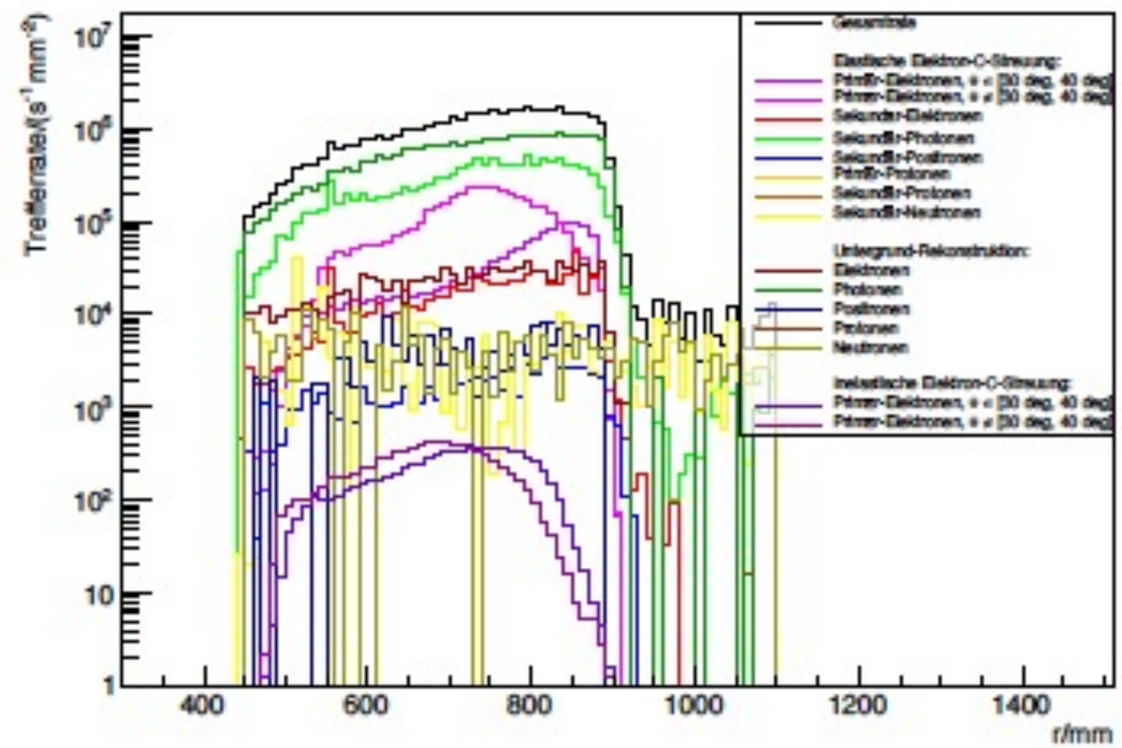

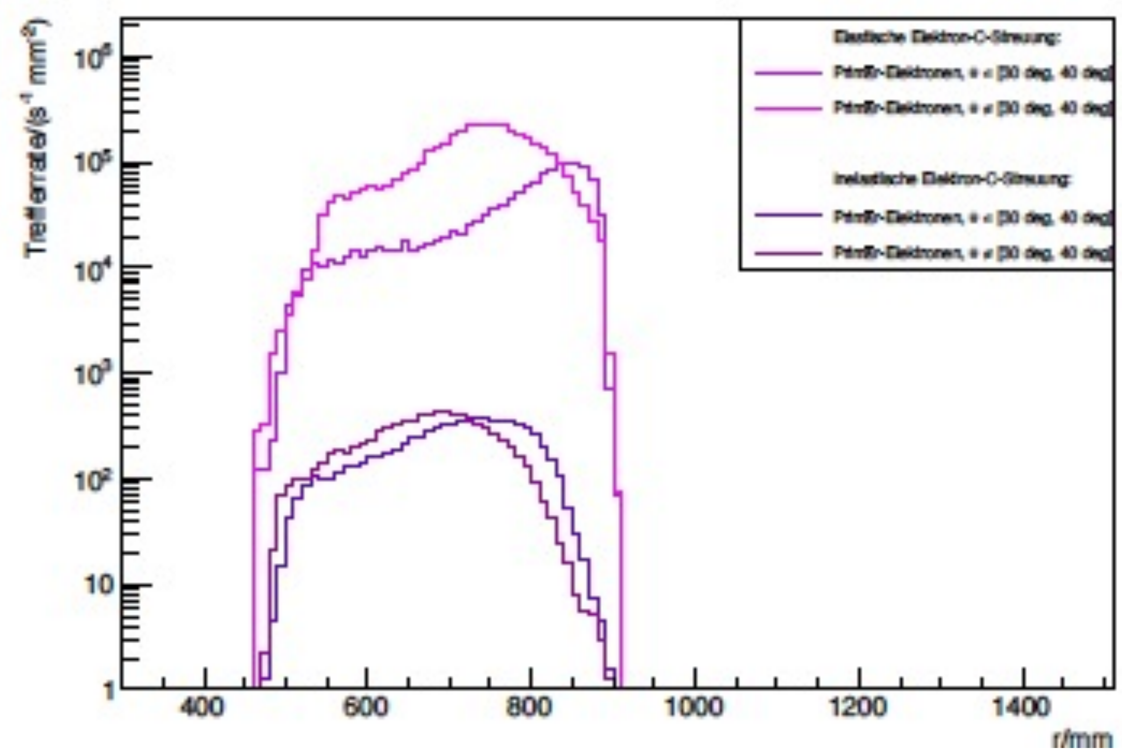

Carbon simulations

- Inelastic scattered electrons
  - Sum from 4.4, 7.6, 9.6 MeV states
  - Located at smaller *r*
- Rate dominated by photons
- Photoelectron rate dominated by primary electrons
- Separation between elastic/inelastic electrons possible

⇒ Use short bars

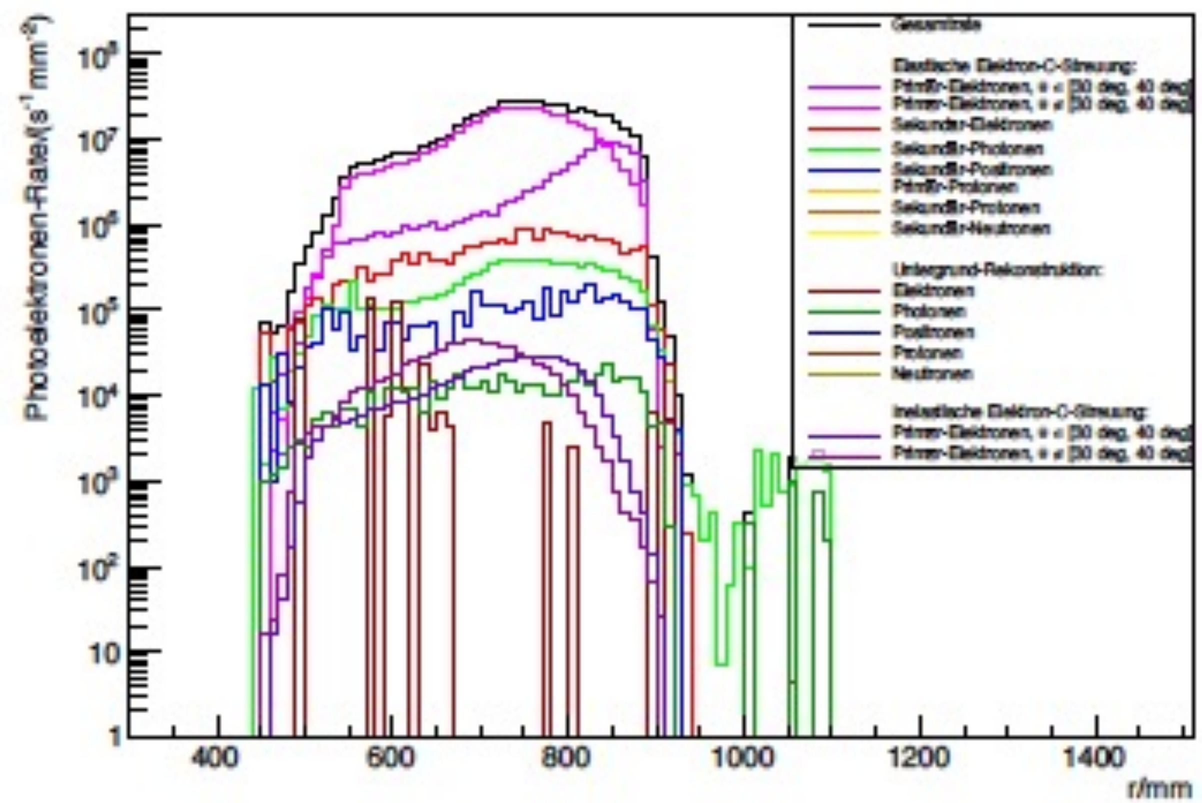

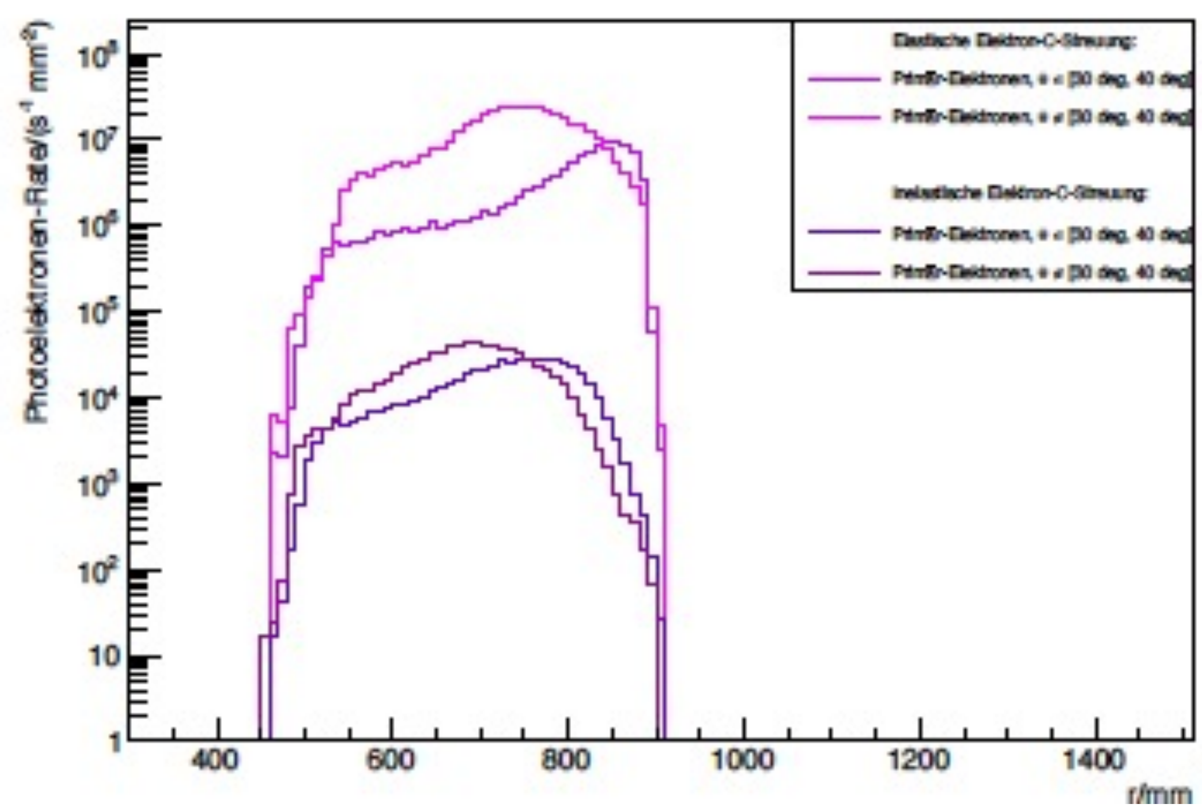

Carbon simulations

- Only elastic scattering
- Asymmetry for inelastic not known
- $P_{\text{beam}} = 85\,\%$
- Asymmetry $A = -\frac{G_f Q^2}{4\sqrt{2}\pi\alpha}\frac{Q_W}{6}$
- For $T = 2500\,\text{h}$:
  - $A_{exp}(650\,\text{mm}) = 353.94 \pm 0.70\,\text{ppb}$
  - $A_{exp}(260\,\text{mm}) = 463.8 \pm 1.6\,\text{ppb}$

Length (mm)	Statistical uncertainty 500 h	1000 h	2000 h	2500 h
250	0.92%	0.63%	0.45%	0.39%
260	0.77%	0.55%	0.40%	0.35%
300	0.57%	0.40%	0.29%	0.26%
400	0.46%	0.32%	0.22%	0.20%
650	0.42%	0.29%	0.21%	0.20%

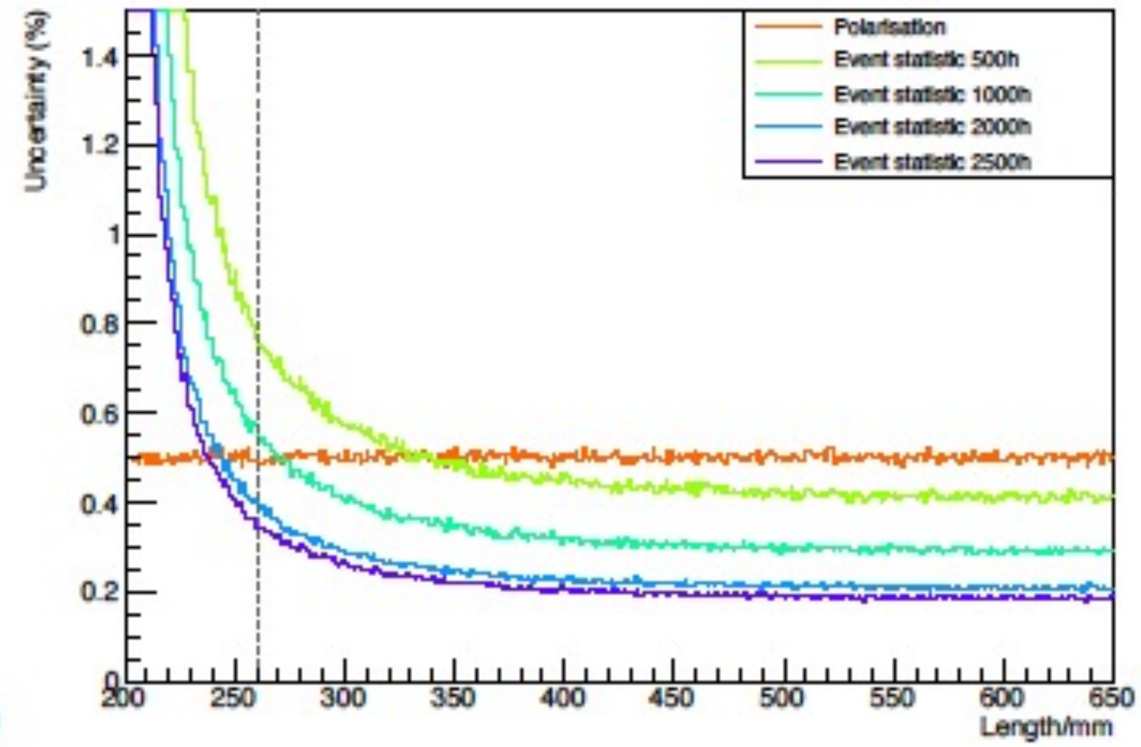

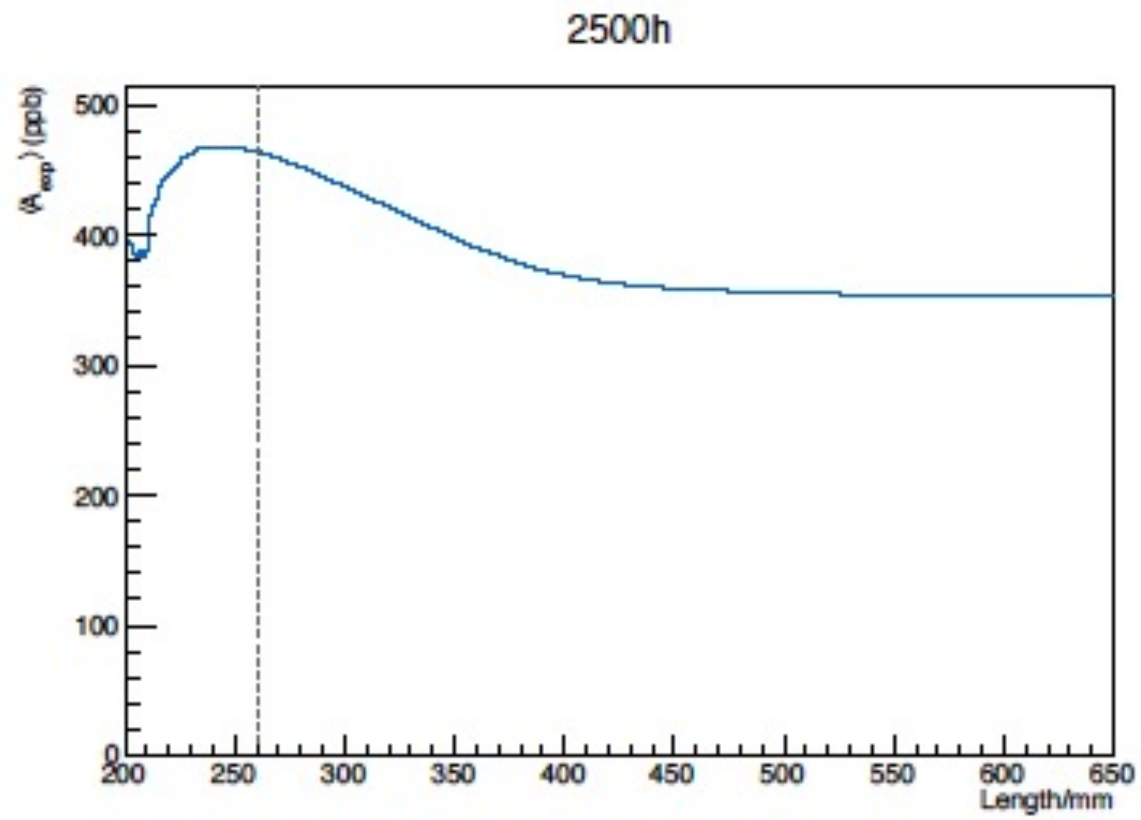

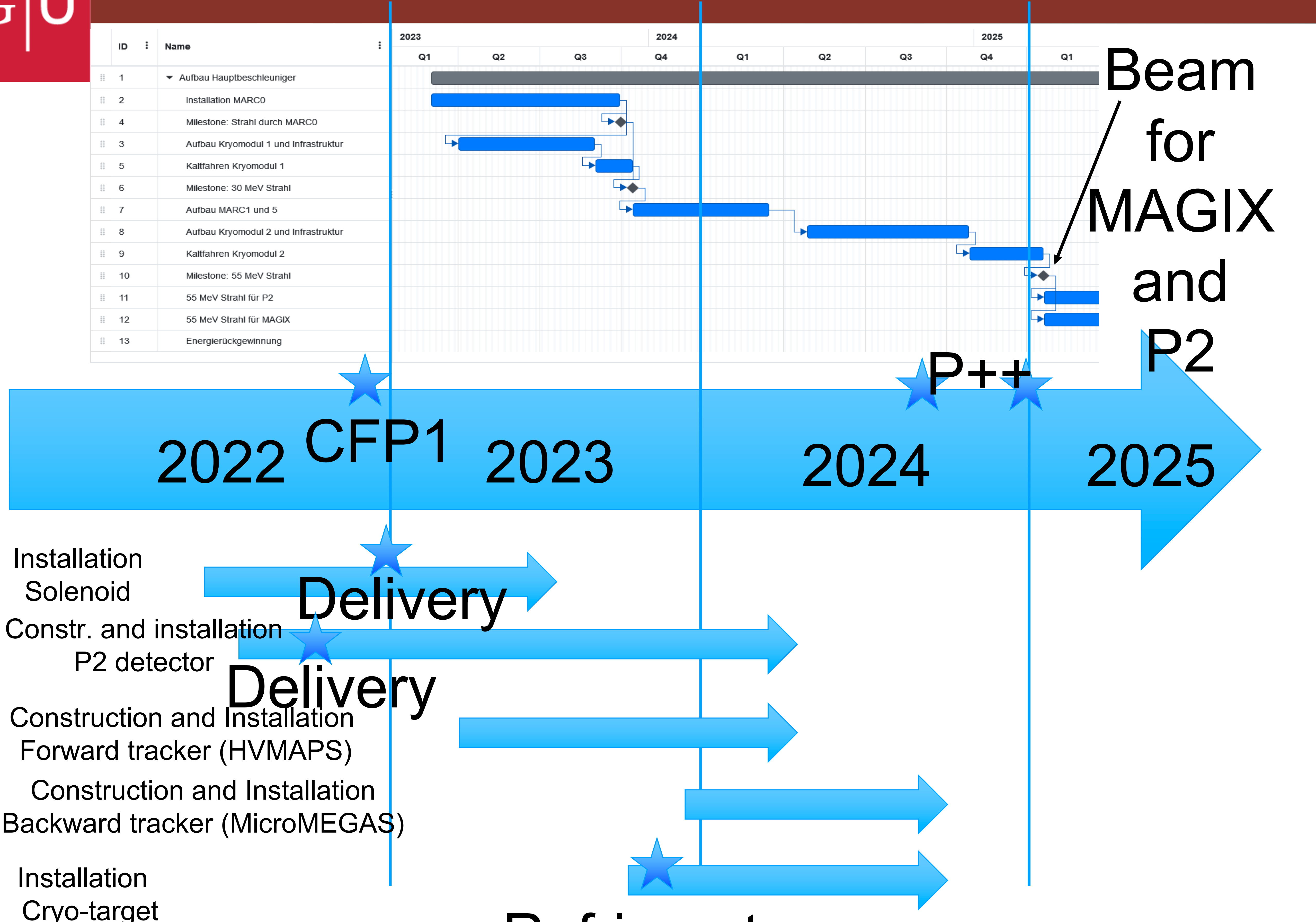

ID
Name
2023
2024
2025
Q1
Q2
Q3
Q4
Q1
Q2
Q3
Q4
Q1
1 Aufbau Hauptbeschleuniger
2 Installation MARC0
4 Milestone: Strahl durch MARC0
3 Aufbau Kryomodul 1 und Infrastruktur
5 Kaltfahren Kryomodul 1
6 Milestone: 30 MeV Strahl
7 Aufbau MARC1 und 5
8 Aufbau Kryomodul 2 und Infrastruktur
9 Kaltfahren Kryomodul 2
10 Milestone: 55 MeV Strahl
11 55 MeV Strahl für P2
12 55 MeV Strahl für MAGIX
13 Energierückgewinnung
Beam for MAGIX and P2
P++
2022
CFP1
2023
2024
2025
Installation Solenoid
Delivery
Constr. and installation P2 detector
Delivery
Construction and Installation Forward tracker (HVMAPS)
Construction and Installation Backward tracker (MicroMEGAS)
Installation Cryo-target
Refrigerator

Summary

- P2-experiment from R&D-Phase to Construction-Phase
  - Main components in Mainz by end of 2022
- P2 will be ready to take data after 2024

- Commissioning of accelerator and the two main experiments in the same hall in parallel (MESA, MAGIX, P2)

- Worlds most precise measurement of parity violating ep, eC, and ePb scattering